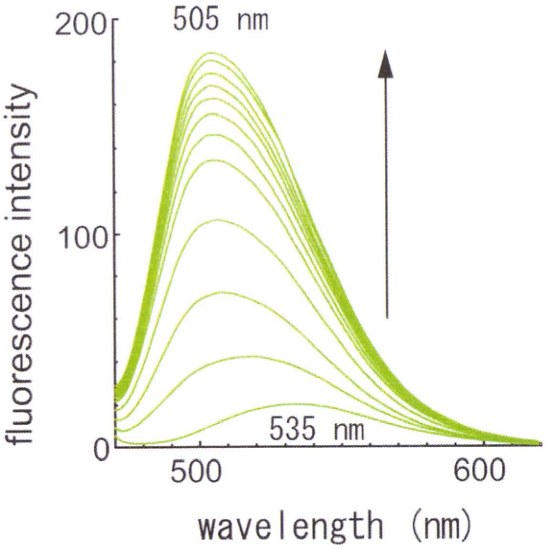

FIGURE 3 Fluorescence spectral change of the probe peptide upon the addition of the tag peptide at 25 C in 50 m*M* HEPES buffer (pH 7.2, 100 m*M* NaCl): [probe] = 0.5 μM, [tag] = 0 to 2.0 μM.

ing of the antiparallel 3α-helical peptide bundle structure is formed as a result of the affinity of the tag peptide and the probe peptide. Since this interaction involves noncovalent bonds, introduction of crosslink by a covalent bond might increase chemical and biological stability. Thus, we developed tag-probe pairs, crosslinked by covalent bonds (see Figure 5).

RESULTS AND DISCUSSTION

Crosslinking Reaction of the Tag Peptide With the Probe Peptide

To investigate the optimum length of crosslinkers, three types of probe peptides with linkers of different lengths were synthesized. The original tag peptide has a side-chain thiol group in the Gly-Gly-Cys-Gly-Gly loop structure between antiparallel 2α-helical peptides. At the N-terminus of each probe peptide, 0, 1, or 2 Gly residues were attached as a spacer and an N^{α}-chloroacetyl group as a functional group for coupling with the Cys thiol group (see Figure 6). The probe peptides having 0, 1, and 2 Gly residues were designated probe **1**, **2**, and **3**. As control probe peptides, probe peptide **4**, which has no chloroacetyl group, and **5**, which has N^{ε}-chloroacetyl-Lys at the C-terminus, both possessing N^{α}-acetyl-Gly, were also prepared. Probe peptides **1**-**5** were prepared by Fmoc-based solid-phase peptide synthesis.[26] The tag peptide was prepared by native chemical ligation[27,28] of the synthetic C-terminal thioester fragment A and the N-terminal cysteine fragment B, which were divided at the cysteine residue of the loop sequence.[20] Using the probe peptides **1**-**3**, the crosslinking reactions with the tag peptide, monitored by HPLC,[29] were performed by addition of the tag peptide to the probe peptide (1:1, final 1 μM each) in 50 m*M* HEPES buffer, pH 7.2 containing 100 m*M* NaCl at room temperature. The time course of the crosslinking reaction of the probe peptide **2** is shown in Figures 7 and 8a. Peak areas of the tag peptide and the probe peptide **2** with the retention times of ~18 min and 32 min, respectively, decreased in a time-dependent manner, while that of the product of crosslink, the tag-probe **2** complex, with retention time of 28 min, increased. Completion of this reaction was the fastest of the crosslinking reactions, requiring approximately 20 min (Figure 8b). The order of the reaction rate of the probe peptides was **2**, **1**, **3**, and **5** (Figures 8b and 9). Reactions of **1** and **3** were mostly complete in 30 min, and the crosslinking reaction of the tag peptide with the probe peptide **5** failed (see Figure 9). These results suggest that a Gly residue at position 1 is the most suitable spacer and that the chloroacetyl group of the probe peptide and the thiol group of the tag peptide react in a structure-specific manner. In the use of the probe peptides **1**-**3** to form the tag-probe pairs, the chloroacetyl and thiol groups approach one another prior to the cross-

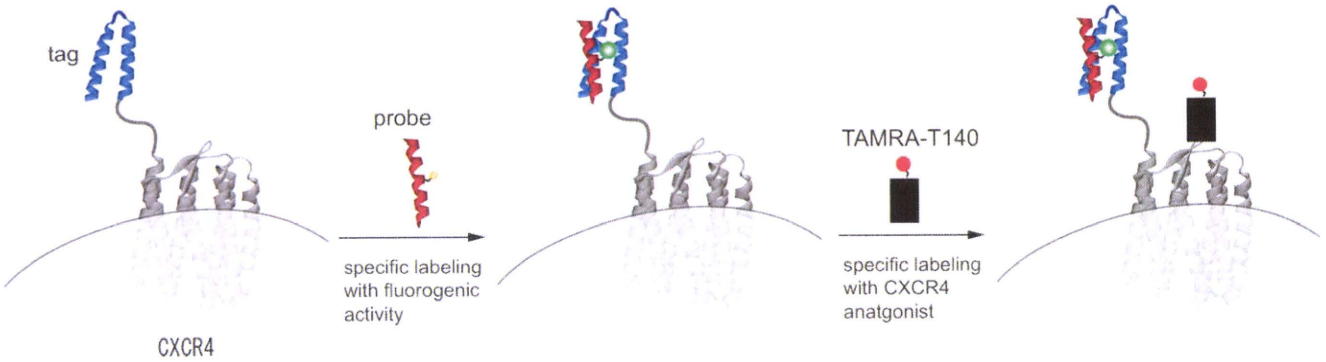

FIGURE 4 Sequential labeling of the tag-fused CXCR4 on the cell surface by the TAMRA-appended CXCR4 antagonist T140 after the labeling by the probe peptide.

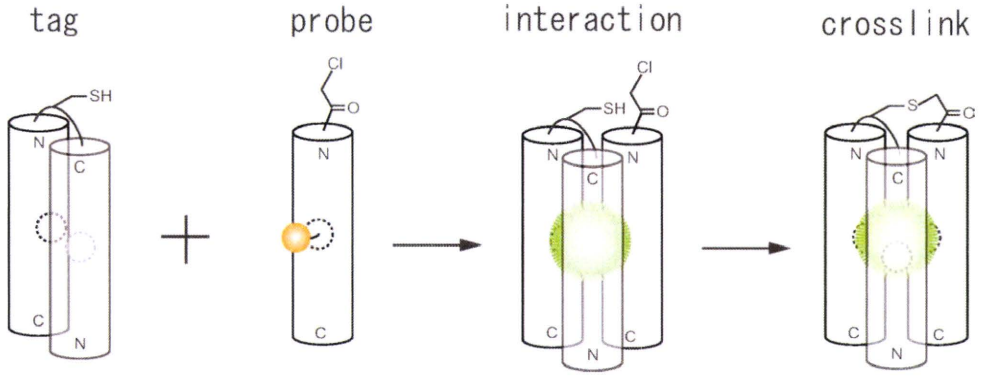

FIGURE 5 Crosslink-type ZIP tag-probe pairs with fluorogenic activity: formation of tag-probe pairs and the subsequent crosslink by a covalent bond.

linking reaction. In the case of the probe peptide **5**, when the tag-probe pair is formed the chloroacetyl and thiol groups are located quite separately on opposite sides and can not interact. All of the crosslink products were purified by RP-HPLC and characterized by ESI-MS.

Fluorescent Titration Analysis

In the fluorescent titration analysis of the addition of the tag peptide to the probe peptide **2**, the fluorescence spectra of **2** changed remarkably, depending on the concentration of the tag peptide. The emission maximum due to the NBD dye showed a significant blue shift from 537 nm to 504 nm with a 22-fold increase in the emission intensity (see Figure 10). Such a spectral change clearly suggests that the NBD moiety of the probe peptide is located in the hydrophobic environment inside the 3α-helical peptide bundle structure, as in noncovalent type formation of the ZIP tag-probe pair.[20] Comparison with the other probe peptides in the fluorescent titration analysis is shown in Figure 10b and Table I. In the use of all of the probe peptides, a similar blue shift of the emission maximum due to the NBD dye from 534–537 nm to 504 nm was observed. The increase of emission intensity, most remarkable in the case of probe peptide **2**, was in the order **2**, **1**, **3**, **4**, and **5**. This suggests that tag-probe **2** pair is most suitable for analytical purposes.

The dissociation constants of the probe peptides **1**, **2**, **3**, **4**, and **5** toward the tag peptide were estimated by analysis using nonlinear least-squares curve fitting[22] as 6.2 n*M*, 6.5 n*M*, 9.0 n*M*, 22 n*M*, and 12 n*M*, respectively (Table I). Thus, in terms of dissociation constant, the probe peptide **1** is comparable to **2**, indicating similar binding affinities, but the hydrophobic environment formed by the interaction of the tag peptide with the probe peptide **2** would appear to be more suitable for the fluorescence emission of the NBD dye.

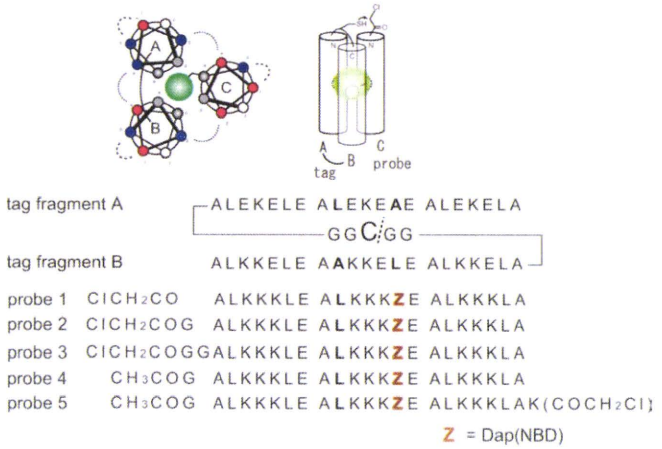

FIGURE 6 Design and structure of crosslink-type ZIP tag-probe pairs. Probe peptides **1**-**3** have an N^{α}-chloroacetyl group at the N-terminus. Probe peptides **4** and **5** have an N^{α}-acetyl group at the N-terminus. Probe peptide **5** has N^{ε}-chloroacetyl-Lys at the C-terminus.

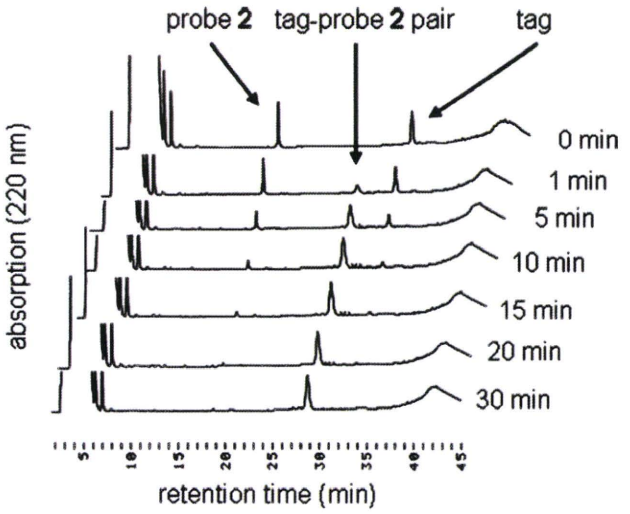

FIGURE 7 HPLC monitoring of the crosslinking reaction of the tag peptide with the probe peptide **2**. The reaction was performed by addition of the tag peptide to the probe peptide **2** (1:1, final 1 μ*M* each) in 50 m*M* HEPES buffer, pH 7.2 containing 100 m*M* NaCl at room temperature.

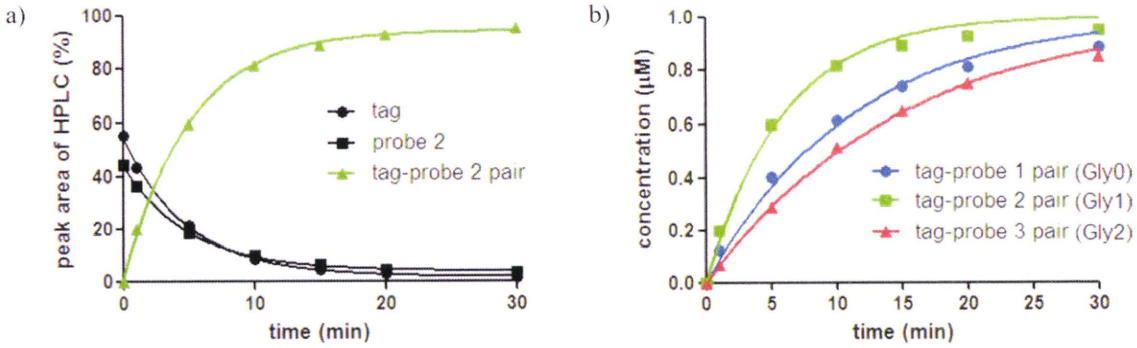

FIGURE 8 The time course of the crosslinking reaction of the tag peptide with the probe peptides. (a) The time course of HPLC peak areas of tag, probe **2** and tag-probe **2** pair, (b) the time course of concentrations of resulting tag-probe **1**-**3** pairs.

Compared with the noncovalent tag-probe **4** pair, whose dissociation constant is 22 n*M*, the affinities of the covalent type tag-probe **1**, **2**, and **3** pairs are remarkably higher, suggesting that crosslink of tag and probe peptides underlies the increase in affinity. In the tag-probe **5** pair, a similar spectral change was observed, indicating that the NBD dye was located in the hydrophobic pocket, although a covalent bond for crosslink of tag and probe peptides was apparently absent (see Figure 11).

Fluorescence Job's Titration

Fluorescent Job's titration, recording the intensity at 505 nm, was performed to assess the stoichiometry of the tag-probe **2** complex (see Figure 12). The total concentration of the probe peptide **2** and the tag peptide was fixed at 1.0 μM. The concentrations of the tag peptide were 0, 0.2, 0.4, 0.5, 0.6, 0.8, and 1.0 μM. This fluorescence Job's titration experiment clearly indicates that the probe peptide **2** binds to the tag peptide with 1:1 stoichiometry. The result suggests that the tag peptide and the probe peptides **1**-**3** form a stable 3α-helical leucine zipper structure by binding with 1:1 stoichiometry.

Investigation of Chemical Stability by Fluorescence Analysis

The chemical stability to thermal denaturation of the tag-probe complexes was investigated. Using the complexes of the tag peptide and the probe peptides **1**-**5**, changes of fluorescence intensity were monitored. The aqueous solution of 1 μM tag-probe complex in 50 m*M* HEPES buffer, pH 7.2 containing 100 m*M* NaCl was prepared, and then the temperature of the solution was gradually increased to 100°C. Fluorescence spectral changes of the tag-probe peptide **2** and **4** pairs, representatives of crosslink pairs and noncrosslink pairs, are shown in Figure 13. In Figure 14 changes of fluorescence intensity of the tag-probe peptide **1**-**5** pairs are shown. In each of the complexes of the tag peptide with probe peptides **1**-**5**, a gradual

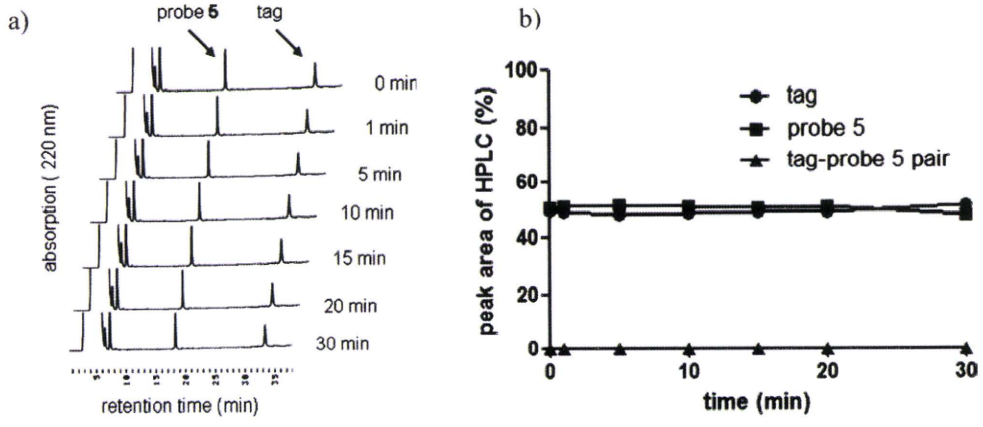

FIGURE 9 (a) HPLC monitoring of the crosslinking reaction of the tag peptide with the probe peptide **5**. The reaction was performed by addition of 1 μM tag peptide to 1 μM probe peptide **5** in 50 m*M* HEPES buffer, pH 7.2 containing 100 m*M* NaCl at room temperature. (b) The time course of HPLC peak areas of tag, probe **5** and tag-probe **5** pair.

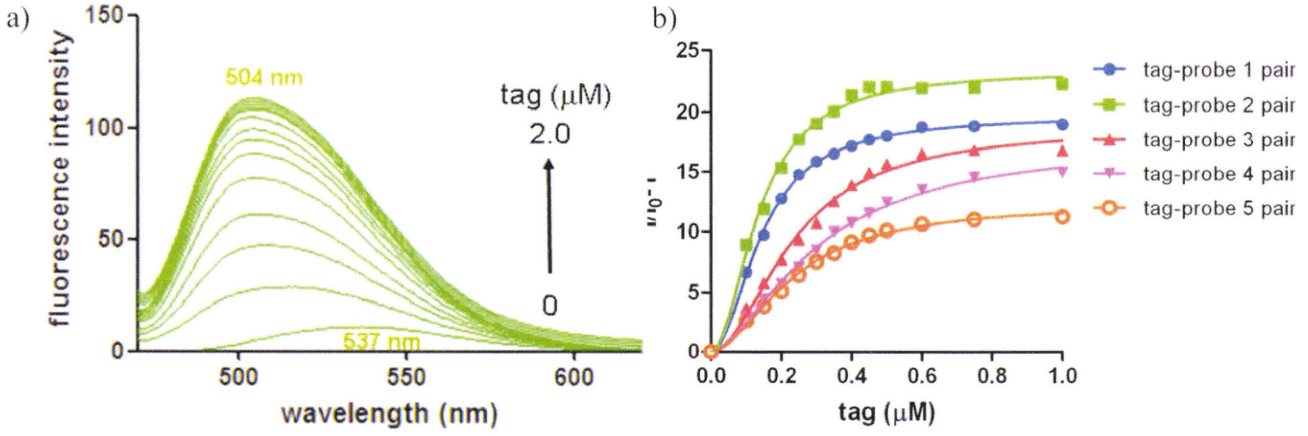

FIGURE 10 (a) Fluorescence spectral change of the probe peptide **2** upon the addition of the tag peptide at 25°C in 50 m*M* HEPES buffer (pH 7.2, 100 m*M* NaCl): [probe] = 0.5 μM, [tag] = 0 to 2.0 μM. (b) Change of fluorescence intensity of the probe peptides **1**-**5** upon the addition of the tag peptide for calculation of dissociation constants of tag-probe pairs.

decrease in fluorescence intensity was observed in proportion to the increase of temperature. The complexes of the tag peptide and the probe peptides **1**-**3** were more stable than those of **4** and **5**, which were completely denatured at 100°C, but the complexes using **1**-**3** were not denatured, possibly due to the crosslinking. The melting temperatures of the complexes using **1**-**3** were above 69°C, whereas those of the complexes involving **4** and **5** were below 56°C.

The possibility that this thermal denaturation is reversible was next investigated. The pairs of tag-probe **2** and tag-probe **4** were adopted as representative of crosslink pairs and non-crosslink pairs, respectively. After denaturing the tag-probe **2** pair at 100°C, the temperature of the solution was gradually decreased (Figure 15a). In proportion to the decrease of temperature, a gradual increase in fluorescence intensity of probe **2** was observed, resulting finally in complete recovery of the original fluorescence intensity. In contrast, while a gradual increase in fluorescence intensity, proportionate to a decrease in temperature, was also observed after the thermal denaturation at 100°C of tag-probe pair **4**, the fluorescence intensity recovered only to approximately half of its original level (Figure 15b). These results suggest that the crosslinking of tag and probe peptides is critical for complete reversibility of the fluorescence emission.

Table I Results of Fluorescence Titration of Tag-Probe Pairs

	Fluorescence Wavelength of Emission Maximum (nm)	I_{max}/I_0 (Fold)	Dissociation Constant (n*M*)[a]
Tag-probe **1** pair	537–504	19	6.2
Tag-probe **2** pair	537–504	23	6.5
Tag-probe **3** pair	535–504	17	9.0
Tag-probe **4** pair	534–504	15	22
Tag-probe **5** pair	534–504	11	12

[a] Measurement conditions: 50 m*M* HEPES buffer solution (pH 7.2, 100 m*M* NaCl), at 25°C, [probe] = 0.5 μM.

Investigation of Chemical Stability by Circular Dichroism

The chemical stability of the tag-probe complexes to thermal denaturation was investigated by circular dichroism (CD). The CD spectra showed that all of the tag-probe **1**-**4** complexes form α-helical structures. The CD spectrum of the tag-probe **2** complex had the strongest double minima at 207 and 222 nm, while the spectrum of the non-covalent type tag-probe **4** complex showed the weakest double minima among the four complexes (see Figure 16). This result sug-

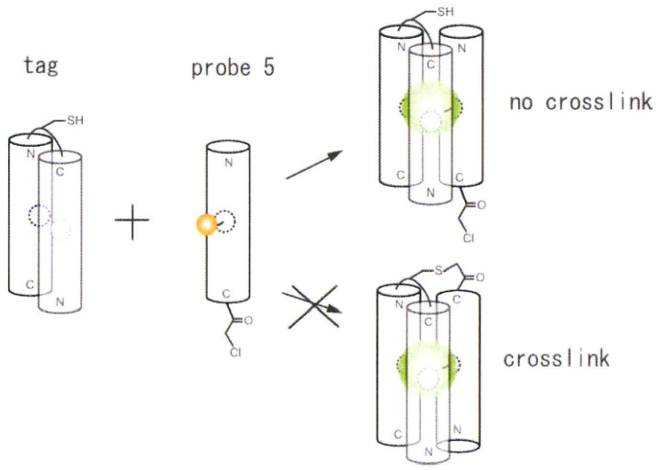

FIGURE 11 Formation of tag-probe **5** pair without crosslinking. When tag-probe **5** pair is formed, the chloroacetyl and thiol groups are separated, located on opposite sides and no covalent bond can form between them.

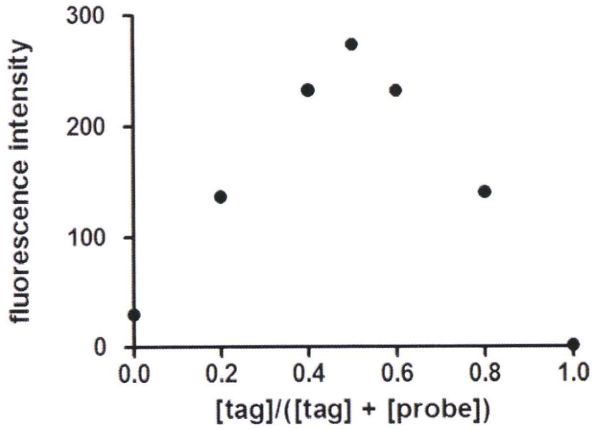

FIGURE 12 Fluorescence Job's titration between the probe peptide **2** and the tag peptide, [probe **2**] + [tag] = 1.0 μM, in 50 mM HEPES buffer (pH 7.2, 100 mM NaCl) at 25 C.

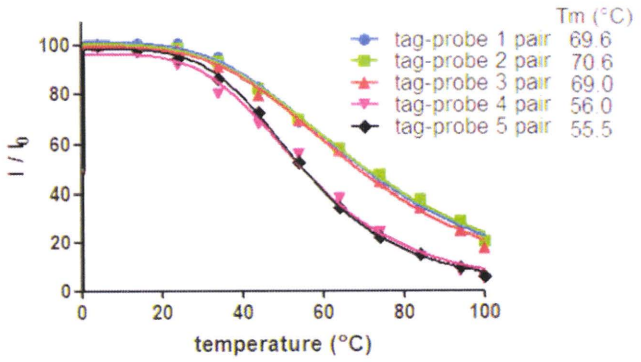

FIGURE 14 Change of fluorescence intensity of tag-probe **1**-**5** pairs from 4°C to 100°C in 50 mM HEPES buffer (pH 7.2, 100 mM NaCl): [tag-probe pair] = 0.5 μM. Values of melting temperature (T_m) of tag-probe peptide **1**-**5** pairs are shown.

gests that crosslinking of the tag and probe peptides is essential for the α-helical structures. Changes in $[\theta]$ at 222 nm in aqueous solution of 1 μM tag-probe pair in 50 mM Tris-HCl buffer, pH 7.2 containing 100 mM NaCl were monitored, and the temperature of the solution was gradually increased to 94°C (Figure 17a). In all the tag-probe **1**-**4** pairs, a gradual increase in values of $[\theta]$ at 222 nm was observed in proportion to the increase in temperature. Tag-probe **4** pair, in particular, showed a remarkable increase in values of $[\theta]$ at 222 nm, suggesting that the α-helical structures were largely collapsed. Judging by the changes of $[\theta]$ at 222 nm, the α-helical structures of tag-probe **1**-**3** pairs survived better than those of tag-probe **4** pair, possibly due to the crosslinking. Next, whether the above α-helical structures can be reversibly recovered was investigated (Figure 17b). The pairs of the tag peptide and the probe peptides **2** and **4** were adopted as representatives of crosslink pairs and noncrosslink pairs, respectively. After denaturing the tag-probe **2** and **4** pairs at 94°C, the temperature of the solution was gradually decreased., Gradual decreases in values of $[\theta]$ at 222 nm in proportion to the decrease of temperature were observed with both pairs. In the case of the tag-probe **2** pair the value of $[\theta]$ at 222 nm was finally nearly completely recovered but with the tag-probe **4** pair $[\theta]$ was not reduced to its original value, suggesting that the crosslink of tag and probe peptides is indispensable for complete reversibility of the α-helical structures.

CONCLUSION

The novel tag-probe pairs based on leucine zipper peptides, in which the thiol group of the Cys residue of the tag peptide and the chloroacetyl group of the probe peptide were crosslinked, have been studied. They were found to have significant fluorogenic activity, mediated by the binding of the tag peptide to the probe peptide as the noncrosslink-type pairs. Compared with noncrosslinked tag-probe pairs, those that are crosslinked were shown to have some advantages in terms of fluorescence

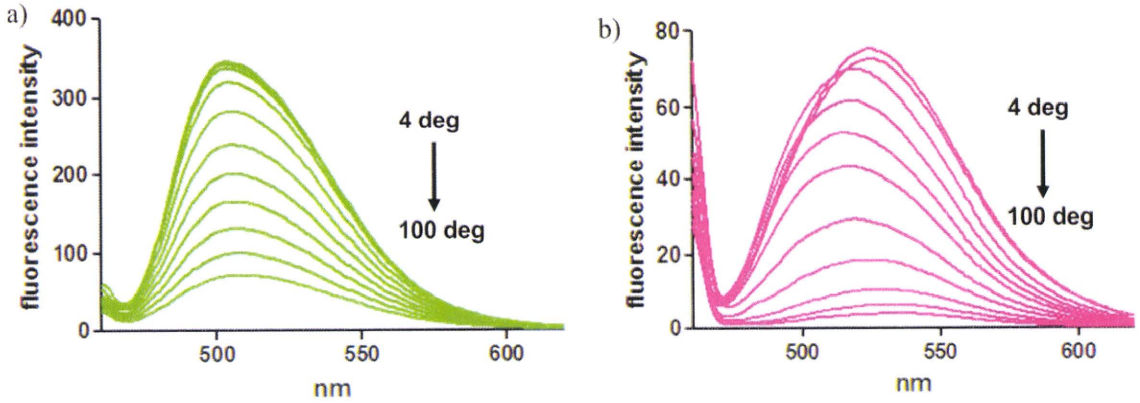

FIGURE 13 Fluorescence spectral change of tag-probe pairs from 4°C to 100°C in 50 mM HEPES buffer (pH7.2, 100 mM NaCl): [tag-probe pair] = 0.5 μM. (a) tag-probe **2** pair, (b) tag-probe **4** pair.

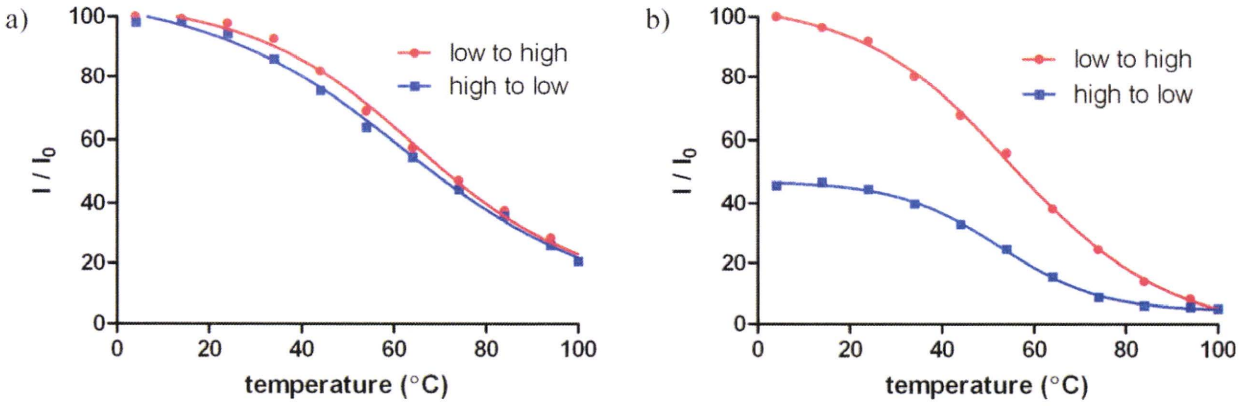

FIGURE 15 Change of fluorescence intensity of tag-probe pairs from 4°C to 100°C (low to high) and from 100°C to 4°C (high to low) in 50 m*M* HEPES buffer (pH 7.2, 100 m*M* NaCl): [tag-probe pair] = 0.5 μM. (a) tag-probe **2** pair, (b) tag-probe **4** pair.

response, binding affinity, and chemical stability. As a spacer between the N^{α}-chloroacetyl group and the original probe sequence, a single Gly residue was superior to 0 or 2 Gly residues. Thus, the probe peptide **2**, having the 1 Gly spacer, binds more rapidly to the tag peptide than the probe peptides **1** and **3**, with 0 and 2 Gly spacers, respectively. Both the previous noncrosslink-type and the present crosslink-type ZIP tag-probe pairs might facilitate the real-time imaging of target proteins without removal of excess probe molecules. Thus, the crosslink-type ZIP tag-probe pairs should be highly useful and valuable for studies of imaging of proteins in living cells.

EXPERIMENTAL PROCEDURES

General

HPLC was carried out on a reversed phase column with a LaChrom Elite HTA system (Hitachi). Matrix-assisted laser desorption/ionization time-of-flight mass spectrometry (MALDI-TOF-MS) was recorded on a Voyager DE-STR (Applied Biosciences) mass spectrometer. 3,5-dimethoxy-4-hydroxycinnamic acid was used as the matrix.

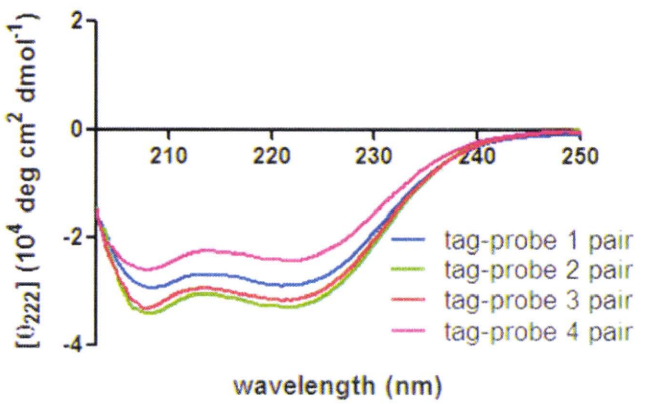

FIGURE 16 CD spectra of tag-probe pairs at 24°C in 50 m*M* Tris-HCl buffer (pH7.2, 100 m*M* NaCl): [tag-probe pair] = 1 μM. Tag-probe peptide **1** pair (blue), tag-probe peptide **2** pair (green), tag-probe peptide **3** pair (red) and tag-probe peptide **4** pair (magenta).

Peptide Synthesis

Probe peptides **1-5** were synthesized by the Fmoc-based solid-phase method.[26] The tag peptide was prepared previously.[20] All peptides were purified by RP-HPLC and identified by MALDI-TOF-MS. Fmoc-protected amino acids and reagents for peptide synthesis were purchased from Novabiochem, Kokusan Chemical Co., Ltd. and Watanabe Chemical Industries, Ltd. Fmoc-Dap(NBD)-OH was synthesized as previously reported.[30] The probe peptides **1-5** were synthesized using NovaSyn TGR resin on a 0.1 mmol scale. All peptides were synthesized by stepwise elongation techniques of Fmoc-protected amino acids on the resin. The coupling reactions were performed using 5.0 equiv. of Fmoc-protected amino acid, 5.0 equiv. of diiopropylcarbodiimide (DIPCI) and 5.0 equiv. of 1-hydroxybenzotriazole monohydrate ($HOBt \cdot H_2O$) in DMF (5.0 mL). N-Terminal amino groups of the probe peptides **1-3** were chloroacetylated with chloroacetic acid, DIPCI and HOBt (5.0 equiv. each) in DMF (5.0 mL). N-Terminal amino groups of the probe peptides **4** and **5** were acetylated with acetic anhydride-DMF (1:4, v/v) (5.0 mL). In the synthesis of the probe peptide **5**, Fmoc-Lys(Mtt)-OH (Mtt = 4-methyltrityl) was coupled as the C-terminal Fmoc-protected amino acid. After construction of the protected peptide **5** resin and N-terminal acetylation, the peptide **5** resin was treated by dichloromethane-triisopropylsilane-TFA (94:5:1, v/v) (2.0 mL) for 1 min, and this treatment was repeated 11 times,[31] followed by N^{ε}-chloroacetylation with chloroacetic acid, DIPCI and HOBt (5.0 equiv. each) in DMF (5.0 mL). Cleavage and side chain deprotection of the probe peptides **1-5** was carried out with 10 mL of TFA in the presence of 0.25 mL of *m*-cresol, 0.75 mL of thioanisole, and 0.75 mL of 1,2-ethanedithiol as scavenger, by stirring for 1.5 h. After filtra-

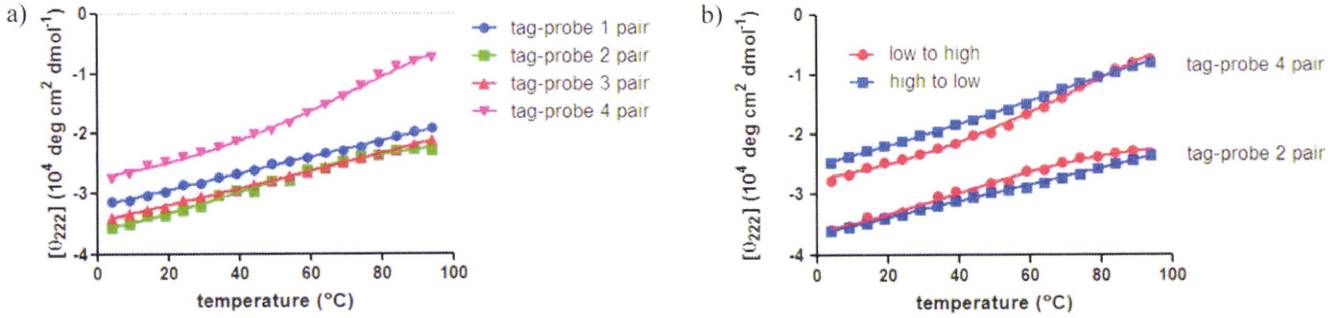

FIGURE 17 (a) Change of values of $[\theta]$ at 222 nm of tag-probe pairs from 4°C to 94°C in 50 m*M* Tris-HCl buffer (pH 7.2, 100 m*M* NaCl): [tag-probe pair] = 1 μM. Tag-probe **1** pair (blue), tag-probe **2** pair (green), tag-probe **3** pair (red) and tag-probe **4** pair (magenta). (b) Change of values of $[\theta]$ at 222 nm of tag-probe **2** and **4** pairs from 4°C to 94°C (low to high) (red) and from 94°C to 4°C (high to low) (blue) in 50 m*M* Tris-HCl buffer (pH 7.2, 100 m*M* NaCl).

tion, the reaction mixture was concentrated under reduced condition, and crude peptides were precipitated in cooled diethyl ether. All crude peptides were purified by RP-HPLC (column, YMC-Pack ODS-A, 10ϕ × 250 mm). The HPLC solvents employed were water containing 0.1% TFA (solvent A) and acetonitrile containing 0.1% TFA (solvent B). The probe peptides **1**-**5** was purified using a 23%–38% linear gradient of solvent B over 30 min. All purified peptides were identified by MALDI-TOF-MS. All peptides were obtained as TFA salts after lyophilization. Probe peptide **1**, yield 21%, *m/z* 2603.1, calcd 2603.5 $[M + H]^+$. Probe peptide **2**, yield 18%, *m/z* 2661.1, calcd 2660.6 $[M + H]^+$. Probe peptide **3**, yield 23%, *m/z* 2717.1, calcd 2717.6 $[M + H]^+$. Probe peptide **4**, yield 26%, *m/z* 2627.0, calcd 2626.6 $[M + H]^+$. Probe peptide **5**, yield 7%, *m/z* 2773.8, calcd 2773.7 $[M + H]^+$.

Crosslinking Reaction

The probe peptide (16 nmol) and tag peptide (16 nmol) were dissolved in 50 m*M* HEPES buffer, pH 7.2 containing 100 m*M* NaCl (16 mL), and incubated at room temperature in an N_2 atmosphere. At intervals (0, 1, 5, 10, 15, 20, and 30 min), an aliquot (1.6 mL) was sampled and 10% aqueous AcOH (0.4 mL) was added to the aliquot. The reaction was traced by HPLC using a 20%–50% linear gradient of solvent B over 30 min. HPLC peaks of the starting compounds and the generated products were identified by MALDI-TOF-MS: tag-probe peptide **1**, *m/z* 7880.4, calcd 7877.2 $[M + H]^+$. Tag-probe peptide **2**, *m/z* 7935.7, calcd 7934.2 $[M + H]^+$. Tag-probe peptide **3**, *m/z* 7993.8, calcd 7991.3 $[M + H]^+$. The amounts of the starting compounds and the generated products were quantified from the peak areas.

Fluorescence Titration Analysis

Fluorescence spectra were recorded on a JASCO FP-750 spectrometer using a quartz cell. A stock solution of the probe peptide was diluted with 50 m*M* HEPES buffer solution (pH 7.2, 100 m*M* NaCl) to prepare the solution with a final concentration (0.5 μM). The corresponding tag peptide solution was added dropwise to a 0.5 μM of the probe peptide solution and the fluorescence spectra (λ_{ex} = 456 nm) were measured at 25°C. An average value of three measurements was plotted as each point. Fluorescent titration curves (λ_{em} = 537 nm for probe **1** and **2**, 535 nm for probe **3**, and 534 nm for probe **4** and **5**) were analyzed with a nonlinear least-squares curve-fitting method to evaluate K_d values. For measurements of thermal denaturation, fluorescence spectra were recorded every 10°C from 4°C to 100°C after 10-min incubation of tag-probe pairs at each temperature. For measurements in thermal changes from high to low temperature, after 1-h incubation of tag-probe pairs at 100°C, fluorescence spectra were recorded every 10°C until 4°C. Tm values were estimated by a nonlinear least-squares curve-fitting method using GraphPad Prism 5 (MDF Co., Ltd.).

Fluorescence Job's Titration

The fluorescent intensity at 505 nm was recorded on a JASCO FP-750 spectrometer using a quartz cell in 50 m*M* HEPES buffer (pH 7.2, 100 m*M* NaCl) at 25°C. The total concentration of the probe peptide and the tag peptide was fixed at 1.0 μM. The concentrations of the tag peptide were 0, 0.2, 0.4, 0.5, 0.6, 0.8, and 1.0 μM. This fluorescence Job's titration experiment clearly indicates that the probe peptide binds to the tag peptide in a 1:1 stoichiometry.

CD Study

CD were recorded on a J-720WI spectropolarimeter using a quartz cell with 0.1 cm pathlength at 25°C. The stock solutions of tag-probe complexes were prepared and diluted with 50 m*M* Tris-HCl buffer solution (pH 7.2, 100 m*M* NaCl) to

prepare the solutions of a final concentration (1.0 μM). Each spectrum shows an average value of three measurements. For measurements of thermal denaturation, CD spectra were recorded every 5°C from 4°C to 94°C after 10-min incubation of tag-probe pairs at each temperature. For measurements in thermal changes from high to low temperature, after 1-h incubation of tag-probe pairs at 94°C, CD spectra were recorded every 5°C until 4°C.

The authors deeply thank Prof. K. Akiyoshi (Tokyo Medical and Dental Univ.) for allowing access to a CD spectropolarimeter.

REFERENCES

1. Terpe, K. Appl Microbiol Biotechnol 2003, 60, 523–533.
2. Hedhammar, M.; Gräslund, T.; Hober, S. Chem Eng Technol 2005, 28, 1315–1325.
3. Guignet, E. G.; Hovius, R.; Vogel, H. Nat Biotechnol 2004, 22, 440–444.
4. Goldsmith, C. R.; Jaworski, J.; Sheng, M.; Lippard, S. J. J Am Chem Soc 2006, 128, 418–419.
5. Hauser, C. T.; Tsien, R. Y. Proc Natl Acad Sci USA 2007, 104, 3693–3697.
6. Griffin, B. A.; Adams, S. R.; Tsien, R. Y. Science 1998, 281, 269–272.
7. Gaietta, G.; Deerinck, T. J.; Adams, S. R.; Bouwer, J.; Tour, O.; Laird, D. W.; Sosinsky, G. E.; Tsien, R. Y.; Ellisman, M. H. Science 2002, 296, 503–507.
8. Marks, K. M.; Rosinov, M.; Nolan, G. P. Chem Biol 2004, 11, 347–356.
9. Ojida, A.; Honda, K.; Shinmi, D.; Kiyonaka, S.; Mori, Y.; Hamachi, I. J Am Chem Soc 2006, 128, 10452–10459.
10. Chen, I.; Choi, Y.-A.; Ting, A. Y. J Am Chem Soc 2007, 129, 6619–6625.
11. O'Hare, H. M.; Johnsson, K.; Gautier, A. Curr Opin Struct Biol 2007, 17, 488–494.
12. Keppler, A.; Gendreizig, S.; Gronemeyer, T.; Pick, H.; Johnsson, K. Nat Biotechnol 2003, 21, 86–89.
13. Gautier, A.; Juillerat, A.; Heinis, C.; Correa, I. R., Jr.; Kindermann, M.; Beaufils, F.; Johnsson, K. Chem Biol 2008, 15, 128–136.
14. Yin, J.; Liu, F.; Li, X.; Walsh, C. T. J Am Chem Soc 2004, 126, 7754–7755.
15. Los, G. V.; Darzins, A.; Karassina, N.; Zimprich, C.; Learish, R.; McDougall, M. G.; Encell, L. P.; Friedman-Ohana, R.; Wood, M.; Vidurgiris, G.; Zimmerman, K.; Otto, P.; Klaubert, D. H.; Wood, K. V. Promega Cell Notes 2005, 11, 2–6.
16. Tripet, B.; Yu, L.; Bautista D. L.; Wong, W. Y.; Irvin, R. T.; Hodges, R. S. Protein Eng 1996, 9, 1029–1042.
17. Zhang, K.; Diehl, M. R.; Tirrell, D. A. J Am Chem Soc 2005, 127, 10136–10137.
18. Obataya, I.; Sakamoto, S.; Ueno, A.; Mihara, H. Biopolymers 2001, 59, 65–71.
19. Yadav, M. K.; Redman, J. E.; Leman, L. J.; Alvarez-Gutie'rrez, J. M.; Zhang, Y.; Stout, C. D.; Ghadiri, M. R. Biochemistry 2005, 44, 9723–9732.
20. Tsutsumi, H.; Nomura, W.; Abe, S.; Mino, T.; Masuda, A.; Ohashi, N.; Tanaka, T.; Ohba, K.; Yamamoto, N.; Akiyoshi, K.; Tamamura, H. Angew Chem Int Ed 2009, 48, 9164–9166.
21. Lovejoy, B.; Choe, S.; Cascio, D.; McRorie, D. K.; DeGrado, W. F.; Eisenberg, D. Science 1993, 259, 1288–1293.
22. Kuwabara, T.; Nakamura, A.; Ueno, A.; Toda, F. J Phys Chem 1994, 98, 6297–6303.
23. Ward, S. G.; Westwick, J. Biochem J 1998, 333, 457–470.
24. Tamamura, H.; Tsutsumi, H.; Nomura, W.; Tanaka, T.; Fujii, N. Exp Opin Drug Disc 2008, 3, 1155–1166.
25. Nomura, W.; Tanabe, Y.; Tsutsumi, H.; Tanaka, T.; Ohba, K.; Yamamoto, N.; Tamamura, H. Bioconjugate Chem 2008, 19, 1917–1920.
26. Chan, W. C.; White, P. D. In Fmoc Solid Phase Peptide Synthesis: A Practical Approach; Chan, W. C.; White, P. D., Eds.; Oxford University Press: New York, 2000; pp 41–76.
27. Dawson, P. E.; Muir, T.W.; Clark-Lewis, I.; Kent, S. B. H. Science 1994, 266, 776–779.
28. Muir, T. W.; Kent, S. B. H. Annu Rev Biochem 2000, 69, 923–960.
29. Nonaka, H.; Tsukiji, S.; Ojida, A.; Hamachi, I. J Am Chem Soc 2007, 129, 15777–15779.
30. Kamoto, M.; Umezawa, N.; Kato, N.; Higuchi, T. Chem Eur J 2008, 14, 8004–8012.
31. Bourel, L.; Carion, O.; Gras-Masse, H.; Melnyk, O. J Peptide Sci 2000, 6, 264–270.

5356 J. Med. Chem. 2010, 53, 5356–5360
DOI: 10.1021/jm1003528

Journal of
Medicinal
Chemistry
Brief Article

Peptide HIV-1 Integrase Inhibitors from HIV-1 Gene Products

Shintaro Suzuki,[†,#] Emiko Urano,[‡,#] Chie Hashimoto,[†] Hiroshi Tsutsumi,[†] Toru Nakahara,[†] Tomohiro Tanaka,[†] Yuta Nakanishi,[†] Kasthuraiah Maddali,[§] Yan Han,[‡] Makiko Hamatake,[‡] Kosuke Miyauchi,[‡] Yves Pommier,[§] John A. Beutler,[⊥] Wataru Sugiura,[‡] Hideyoshi Fuji,[∥] Tyuji Hoshino,[∥] Kyoko Itotani,[†] Wataru Nomura,[†] Tetsuo Narumi,[†] Naoki Yamamoto,[‡] Jun A. Komano,[‡] and Hirokazu Tamamura*[,†]

[†]*Department of Medicinal Chemistry, Institute of Biomaterials and Bioengineering, Tokyo Medical and Dental University, 2-3-10 Kandasurugadai, Chiyoda-ku, Tokyo 101-0062, Japan,* [‡]*AIDS Research Center, National Institute of Infectious Diseases, 1-23-1 Toyama, Shinjuku-ku, Tokyo 162-8640, Japan,* [§]*Laboratory of Molecular Pharmacology, Center for Cancer Research, National Cancer Institute, National Institutes of Health, Bethesda, Maryland 20892-4255,* [∥]*Department of Physical Chemistry, Graduate School of Pharmaceutical Sciences, Chiba University, 1-33 Yayoi-cho, Inage-ku, Chiba 263-8522, Japan, and* [⊥]*Molecular Targets Laboratory, Center for Cancer Research, National Cancer Institute, National Institutes of Health, Frederick, Maryland 21702.* [#] *These authors contributed equally to this work.*

Received March 17, 2010

Anti-HIV peptides with inhibitory activity against HIV-1 integrase (IN) have been found in overlapping peptide libraries derived from HIV-1 gene products. In a strand transfer assay using IN, inhibitory active peptides with certain sequential motifs related to Vpr- and Env-derived peptides were found. The addition of an octa-arginyl group to the inhibitory peptides caused a remarkable inhibition of the strand transfer and 3′-end-processing reactions catalyzed by IN and significant inhibition against HIV replication.

Introduction

Many antiretroviral drugs are currently available to treat human immunodeficiency virus type 1 (HIV-1) infection. Viral enzymes such as reverse transcriptase (RT[a]), protease and integrase (IN), gp41, and coreceptors are the main targets for antiretroviral drugs that are under development. Because of the emergence of viral strains with multidrug resistance (MDR), however, new anti-HIV-1 drugs operating with different inhibitory mechanisms are required. Following the success of raltegravir, IN has emerged as a prime target. IN is an essential enzyme for the stable infection of host cells because it catalyzes the insertion of viral DNA inside the preintegration complex (PIC) into the genome of host cells in two successive reactions, designated as strand transfer and 3′-end-processing. It is assumed that the enzymatic activities of IN have to be negatively regulated in the PIC during its transfer from the cytoplasm to the nucleus. Otherwise, premature activation of IN can lead to the autointegration into the viral DNA itself, resulting in an aborted infection. We speculate that the virus, rather than the host cells, must encode a mechanism to prevent autointegration. The PIC contains in association with the viral nucleic acid, viral proteins such as RT, IN, capsids ($p24^{CA}$ and $p7^{NC}$), matrix ($p17^{MA}$), p6 and Vpr, cellular proteins HMG I (Y), and the barrier to autointegration factor (BAF).[1−4] It is likely that, due to their spatial proximity in the PIC, these proteins physically and functionally interact with each other. For instance, it is already known that RT activity inhibited by Vpr,[5] and that RT and IN inhibit each other.[5−9] Vpr also inhibits IN through its C-terminal domain.[5,10] Because these studies suggest that PIC components regulate each other's function, we have attempted to obtain potent inhibitory lead compounds from a peptide fragment library derived from HIV-1 gene products, an approach which has been successful in finding a peptide IN inhibitor from LEDGF, a cellular IN binding protein.[11]

In this paper, we describe the screening of an overlapping peptide library derived from HIV-1 proteins, the identification of certain peptide motifs with inhibitory activity against HIV-1 IN, and the evaluation of effective inhibition of HIV-1 replication in cells using the identified peptide inhibitors possessing cell membrane permeability.

Results and Discussion

An overlapping peptide library spanning HIV-1 SF2 *Gag*, *Pol*, *Vpr*, *Tat*, *Rev*, *Vpu*, *Env*, and *Nef*, provided by Dr. Iwamoto of the Institute of Medical Science at the University of Tokyo (Supporting Information, SI, Figure 2A), was screened with a strand transfer assay[12] in search of peptide pools with inhibitory activity against HIV-1 IN. The library consists of 658 peptide fragments derived from the HIV-1 gene products. Each peptide is composed of 10−17 amino acid residues with overlapping regions of 1−7 amino acid residues. Sixteen peptide pools containing between 16 and 65 peptides were used for the first screening at the final concentration of 5.0 μM for each peptide (SI Figure 2B). This initial screening gave the results shown in Figure 1. Both Vpr and Env4 pools showed remarkable inhibition of IN strand transfer activity, and consequently a second screening was performed using the individual peptides contained in the Vpr and Env4 pools. A group of consecutive overlapping peptides in the Vpr pool (groups 13−15) and groups 4−6 and 20−21 in the Env4 pool were found to possess IN inhibitory activity (Figure 2). We focused on Vpr15 and Env4-4 peptides because they showed inhibitory activity against IN strand transfer reaction in a dose-dependent manner (Figure 3). The IC_{50} values of Vpr15

*To whom correspondence should be addressed. Phone: +81-3-5280-8036. Fax: +81-3-5280-8039. E-mail: tamamura.mr@tmd.ac.jp.

[a]Abbreviations: HIV, human immunodeficiency virus; IN, integrase; RT, reverse transcriptase; MDR, multidrug resistance; PIC, preintegration complex; BAF, barrier to autointegration factor; R_8, octa-arginyl.

 Published on Web 06/29/2010

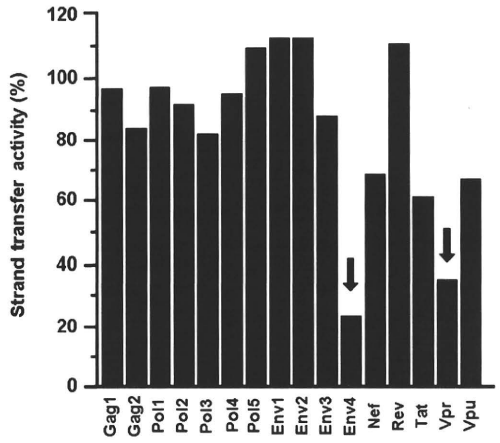

Figure 1. Inhibition of the IN strand transfer activity by peptide pools. Inhibition of the IN strand transfer activity was strongly inhibited by Env4 and Vpr pools (arrows). The *y*-axis represents the IN strand transfer activity relative to the solvent control (DMSO).

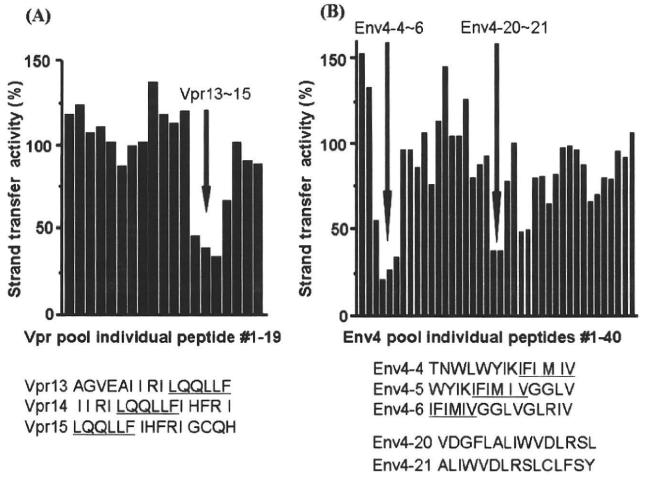

Figure 2. Identification of IN inhibitory peptides in the Vpr (A) and Env4 (B) pools based on the strand transfer activity of IN. The consecutive overlapping peptides display the inhibition of the strand transfer activity of IN (arrows). The *y*-axis represents the IN strand transfer activity relative to the solvent control (DMSO). The concentration of each peptide was 5 μM. The common sequences of individual peptides derived from Vpr and Env4 pools with anti-IN activity are underlined.

and Env4-4 were estimated at 5.5 and 1.9 μM, respectively. These peptides did not show any significant inhibitory activity against HIV-1 RT, suggesting that they might inhibit IN strand transfer reaction selectively.

The overlapping peptides of Vpr13-15 and Env4-4-6 have the vommon hexapeptide sequences LQQLLF and IFIMIV, respectively. The LQQLLF sequence covers positions 64−69 of Vpr, which is a part of the second helix of Vpr. The IFIMIV sequence corresponds to positions 684−689 of gp160, which is a part of the transmembrane domain of TM/gp41. These hexapeptides are thought to be critical to inhibition of IN activity. It was recently reported[5] that similar peptides derived from Vpr inhibit IN with IC_{50} values of 1−16 μM, which is consistent with our data. In this report,[5] the peptide motif was found to be 15 amino acid residues spanning LQQLLF from the overlapping Vpr peptide library. In our study, more precise mapping of inhibitory motif in Vpr peptides was achieved by identifying the shorter effective peptide motif. We focused on the Vpr-derived peptide, LQQLLF (Vpr-1) to develop potent inhibitory peptides. However, the expression of inhibitory activity against IN

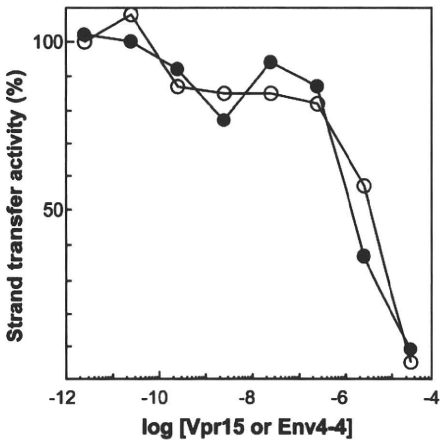

Figure 3. Concentration-dependent inhibition of IN strand transfer activities by Vpr15 (○) and Env4−4 (●) peptides. The *y*-axis represents the IN strand transfer activity relative to the solvent control (DMSO).

in vivo by only hexapeptides might be difficult because these hexapeptides penetrate the plasma membrane very poorly and to achieve antiviral activity, it is essential that they penetrate the cell membrane. To that effect, an octa-arginyl (R_8) group[13] was fused to the Vpr-derived peptides (Table 1). R_8 is a cell membrane permeable motif and its fusion with parent peptides successfully generates bioactive peptides without significant adverse effects or cytotoxicity.[14−18] In addition, the R_8-fusion could increase the solubility of Vpr-derived peptides which have a relatively hydrophobic character.

The inhibitory activity of Vpr-1 and Vpr-1-4 R_8 peptides against IN was evaluated based on the strand transfer and 3′-end-processing reactions in vitro (Table 1).[19,20] Vpr-1 did not show strong inhibition of either IN activity, but the IC_{50} of Vpr-1 R_8 toward the strand transfer reaction of IN was 10-fold lower than that of Vpr-1 lacking the R_8 group. This indicates that the positive charges derived from the R_8 group might enhance the inhibitory activity of the Vpr-1 peptide. Because we were concerned that the strong positive charges close to the LQQLLF motif might interfere with the inhibitory activity, the 6 amino acid sequence (−IHFRIG−) was inserted as a spacer between LQQLLF and R_8 (Vpr-3 R_8). The IHFRIG sequence was used to reconstitute the natural Vpr. The IC_{50} values of Vpr-2 R_8 for the strand transfer and 3′-end-processing activities of IN were 0.70 and 0.83 μM, respectively, while Vpr-3 R_8 showed potent IN inhibitory activities of 4.0 and 8.0 nM against the strand transfer and 3′-end- processing activities, respectively. This result indicates the additional importance of the IHFRIG sequence for inhibitory activities against IN. The increased IN inhibitory activities might be achieved presumably by the synergistic effect of the LQQLLF motif, the IHFRIG sequence, and the R_8 group. Vpr-4 R_8, in which the EAIIRI sequence was attached to further reconstitute the Vpr helix 2, showed inhibitory activities similar to those of Vpr-3 R_8, suggesting that reconstitution of helix 2 of Vpr is not necessary for efficient IN inhibition. Vpr-3 R_8 and Vpr-4 R_8, with $IC_{50} > 0.5\,\mu M$,[21] were less potent inhibitors of RT-associated RNase H activity, indicating that these peptides can selectively inhibit IN. These results suggest that Vpr-derived peptides are novel and distinct from any other IN inhibitors reported to date.

For rapid assessment of the antiviral effect of Vpr-derived peptides, we established an MT-4 Luc system in which MT-4 cells were stably transduced with the firefly luciferase expression cassette by a murine leukemia viral vector (SI Figure 3).

Table 1. Sequences of Vpr-Derived Peptides and Their IC_{50} Values toward the Strand Transfer and 3′-End Processing Reactions of IN

	sequence	IC_{50} (μM) strand transfer	IC_{50} (μM) 3′-end processing
Vpr-1	LQQLLF	68 ± 1.0	> 100
Vpr-1 R_8	Ac-LQQLLF -R_8-NH_2	6.1 ± 1.1	> 11
Vpr-2 R_8	Ac-IHFRIG-R_8-NH_2	0.70 ± 0.06	0.83 ± 0.07
Vpr-3 R_8	Ac-LQQLLF IHFRIG-R_8-NH_2	0.004 ± 0.0001	0.008 ± 0.001
Vpr-4 R_8	Ac-EAIIRI LQQLLF IHFRIG-R_8-NH_2	0.005 ± 0.002	0.006 ± 0.006

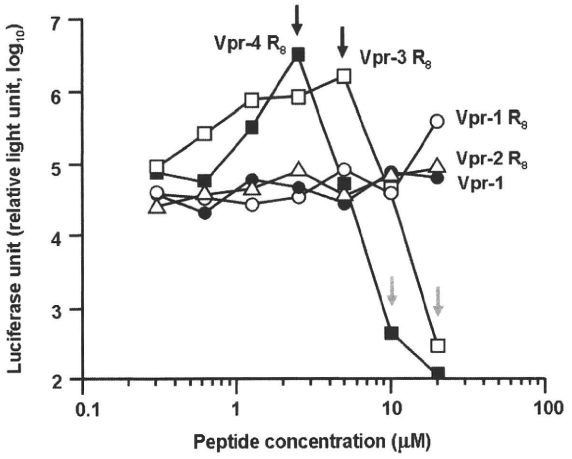

Figure 4. Luciferase signals in MT-4 Luc cells infected with HIV-1 in the presence of various concentrations of Vpr-derived peptides: Vpr-1 (●), Vpr-1 R_8 (○), Vpr-2 R_8 (△), Vpr-3 R_8 (□), Vpr-4 R_8 (■).

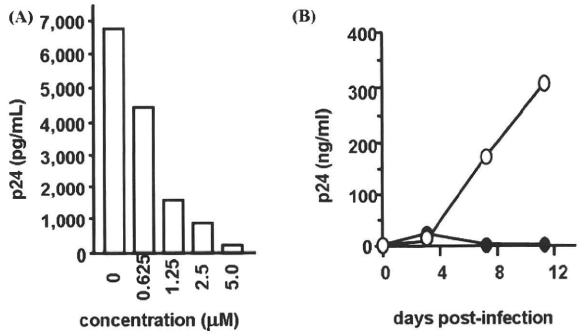

Figure 5. (A) The inhibition of HIV-$1_{JR\text{-}CSF}$ replication in NP2-CD4-CCR5 cells in the presence of various concentrations of Vpr-3 R_8. (B) The replication kinetics of HIV-1_{HXB2} in MT-4 cells in the presence of Vpr-3 R_8 (●). The concentration of Vpr-3 R_8 was fixed at 0.5 μM. Absence of Vpr-3 R_8 (○).

MT-4 Luc cells constitutively express high levels of luciferase which are significantly reduced by HIV-1 infection due to their high susceptibility to cell death upon HIV-1 infection. Protection of MT-4 Luc cells from HIV-1-induced cell death maintains the luciferase signals at high levels. In addition, the cytotoxicity of Vpr-derived peptides can be evaluated by a decrease of luciferase signals in these MT-4 Luc systems. Vpr-2 R_8, which is a weak IN inhibitor, showed no significant anti-HIV-1 activity below concentrations of 20 μM, suggesting that its moderate IC_{50} level in vitro is not sufficient to suppress HIV-1 replication in tissue culture and that the R_8 group is not significantly cytotoxic (Figure 4). Vpr-1 did not show any inhibitory effects against HIV-1 replication; however, Vpr-1 R_8 displayed a weak antiviral effect at a concentration of 20 μM and both Vpr-3 R_8 and Vpr-4 R_8 showed significant inhibitory effects against HIV-1 replication. The R_8 peptide did not show significant anti-HIV activity (IC_{50} > 50 μM, data not shown). These results suggest that the addition of the R_8 group enables Vpr-derived peptides to enter the cytoplasm and access IN, with the result that HIV-1 replication could be effectively inhibited.

Because Vpr-3 R_8 was less cytotoxic than Vpr-4 R_8, the inhibitory activities of Vpr-3 R_8 were further investigated. Two replication assay systems, R5-tropic HIV-$1_{JR\text{-}CSF}$ on NP2-CD4-CCR5 cells and X4-tropic HIV-1_{HXB2} on MT-4 cells, were utilized. NP2-CD4-CCR5 cells were infected with HIV-$1_{JR\text{-}CSF}$ in the presence of various concentrations of Vpr-3 R_8. On day 4 postinfection, the culture supernatant was collected and the concentration of viral p24 antigen was measured by an ELISA assay. The p24 levels decreased in a dose-dependent manner with increasing the concentration of Vpr-3 R_8; 50% inhibition of p24 expression was obtained with approximately 0.8 μM of Vpr-3 R_8 (Figure 5A). This concentration was approximately 10-fold lower than the concentration of Vpr-3 R_8 known to be cytotoxic (Figure 4). Second, MT-4 cells were infected with HIV-1_{HXB2} and the replication kinetics was monitored in the presence of 0.5 μM Vpr-3 R_8. The degree of replication of HIV-1_{HXB2} was quite low in the presence of Vpr-3 R_8, while replication of HIV-1_{HXB2} was robust in the absence of Vpr-3 R_8 (Figure 5B), suggesting that Vpr-3 R_8 strongly suppresses the replication of HIV-1 in cells. To examine whether the HIV-1 replication was blocked through the inhibition of IN activity, quantitative real-time PCR was performed. If IN is inhibited, the efficiency of viral genome integration should be decreased while the reverse transcription of viral genome should not be affected. Accordingly, NP2-CD4-CXCR4 cells were infected with HIV-1_{HXB2} in the presence or absence of 0.5 μM Vpr-3 R_8. Genomic DNA was extracted on day 2 postinfection, and the viral DNA was quantified at the various steps of viral entry phase. The level of "strong stop DNA", representing the total genome of infected virus in Vpr-3 R_8-treated cells, was similar (139.7%) to that in DMSO-treated control cells and the level of viral DNA generated at the late stage of reverse transcription in Vpr-3 R_8-treated cells was slightly decreased (84.4%) compared to control cells. This small decline can probably be attributed to the weak anti-RNase H activity of Vpr-3 R_8. On the other hand, a drastic decrease of Alu-LTR products was observed in Vpr-3 R_8-treated cells (15.8%), indicating an inhibition of integrated viral genome. Concomitantly, the double LTR products, representing the end-joined viral genome catalyzed by host cellular enzymes, were increased by a factor of 8 (779.8%). These results strongly suggest that Vpr-3 R_8 blocks viral infection by inhibiting IN activity in cells, consistent with our in vitro observations. Judging by these results, Vpr-derived peptides with the R_8 group are potent IN inhibitors that suppress HIV-1 replication in vivo.

Finally, in silico molecular docking simulations of Vpr-derived peptides and HIV-1 IN were performed. The Vpr-derived peptides are located in the second helix of Vpr and were thus considered to have an α-helical conformation.[22] Docking simulations of three peptides (Vpr13, Vpr14, and Vpr15), using the predicted structure of the HIV-1 IN dimer as a template,[23] were performed by GOLD software to investigate the binding mode of the peptides, the binding affinity of

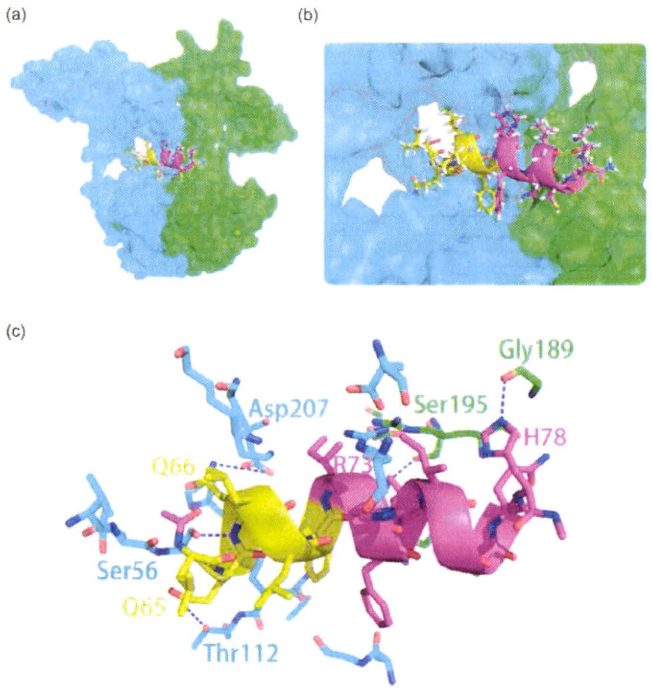

Figure 6. Predicted binding mode of Vpr15 to HIV-1 IN by GOLD. An overall view of (a) the complex obtained by docking Vpr15 with the HIV-1 IN dimer and (b) the closer view of the complex. The predicted structure of full-length HIV-1 IN was used as a template. Each HIV-1 IN monomer was shown as green or cyan surface. The docked Vpr15 is shown as a cartoon. The yellow-colored region is the LQQLLF motif. The GOLD score representing the docking complementarity is 69.83, indicating the high binding affinity between Vpr15 and IN. The hydrogen-bond interactions between HIV-1 IN and Vpr15 were presented by LIGPLOT software shown as blue dotted line (c).

the peptides being evaluated by GOLD Fitness score. The predicted binding mode of Vpr15 to IN is shown in Figure 6. Our results predict that the three Vpr-derived peptides interact with the cleft between the amino-terminal domain and the core domain of HIV-1 IN. This region is distinct from the nucleic acid interacting surfaces, indicating that the Vpr-derived peptides inhibit IN function in an allosteric manner. A previous report provided a model in which a Vpr peptide was bound to IN in a manner similar with our model[5] and, interestingly, the peptides were bound to IN with an exterior surface of Vpr. This earlier report that the full-length Vpr inhibits IN[10] strongly supports the predicted binding mode of Vpr15. Five hydrogen-bond interactions between HIV-1 IN and Vpr15 were identified by LIGPLOT analysis,[24] which invoked the following IN-Vpr amino acids: IN Thr112-Vpr Gln65, IN Ser56-Vpr Gln66, IN Asp207-Vpr Gln66, IN Ser195-Vpr Arg73, and IN Gly189-Vpr His78. The numbering of Vpr amino acids is based on the Vpr full-length coordinate, Figure 6. Additional hydrophobic contacts between IN and Vpr15 were found in which the following IN-Vpr amino acid pairs are involved: IN Lys211-Vpr Gln66, IN Pro109-Vpr Phe69, IN Arg262-Vpr His71, and IN Arg187-Vpr Gln77. These data indicate that the Gln65, Gln66, and Phe69 residues in Vpr-derived peptides play a major role in the interaction between IN and Vpr-derived peptides.

Conclusions

In summary, two peptide motifs, LQQLLF from Vpr and IFIMIV from Env4, possessing inhibitory activity against HIV-1 IN, were identified through the screening of overlapping peptide library derived from HIV-1 gene products. We initially speculate that HIV encodes a mechanism to prevent autointegration in the PIC because integration activity must be regulated until the virus infects cells. This speculation is supported by the finding that IN inhibitors exist in the viral PIC components. Vpr-derived peptides with the R_8 group showed remarkable inhibitory activities against the strand transfer and 3′-end-processing reactions catalyzed by HIV-1 IN in vitro. In addition, Vpr-3 R_8 and Vpr-4 R_8 were shown to inhibit HIV-1 replication with submicromolar IC_{50} values in cells using the MT-4 Luc cell system. In the quantitative analysis of p24 antigen, 50% inhibition of HIV-$1_{JR\text{-}CSF}$ replication was caused by approximately 0.8 μM of Vpr-3 R_8, and the replication of HIV-1_{HXB2} was extensively suppressed in the long term by Vpr-3 R_8 at 0.5 μM concentrations. Our finding suggest that these peptides could serve as lead compounds for novel IN inhibitors. Amino acid residues critical to the interaction of Vpr-derived peptides with IN were identified by our in silico molecular docking simulations, and suggests that more potent peptides[25] or peptidomimetic IN inhibitors represent a novel avenue for future small molecule inhibitors of IN and HIV integration.

Experimental Section

Peptide Synthesis. Vpr-derived peptides containing the R_8 group were synthesized by stepwise elongation techniques of Fmoc-protected amino acids on NovaSyn TGR resin. Coupling reactions were performed using 5.0 equiv of Fmoc-protected amino acid, 5.0 equiv of diisopropylcarbodiimide, and 5.0 equiv of 1-hydroxybenzotriazole monohydrate. Cleavage of peptides from resin and side chain deprotection were carried out with 10 mL of TFA in the presence of 0.25 mL of *m*-cresol, 0.75 mL of thioanisole, 0.75 mL of 1,2-ethanedithiol, and 0.1 mL of water as scavenger by stirring for 1.5 h. After filtration of the deprotected peptides, the filtrate was concentrated under reduced pressure, and crude peptides were precipitated in cooled diethyl-ether. All crude peptides were purified by RP-HPLC and identified by MALDI-TOFMS. Purities of all final compounds were confirmed (>95% purity) by analytical HPLC. Detailed data are provided in SI.

Enzyme Assays. The strand transfer assay for the first screening was performed as described previously.[12] The IN strand transfer and 3′-end-processing assays for peptide motif characterizations were performed as described previously.[19,20] RNase H activity was measured as described by Beutler et al.[21]

Replication Assays. For HIV-1 replication assays, 1×10^5 cells were incubated at room temperature for 30 min with an HIV-1 containing culture supernatant (ca. 0.2−50 ng p24) and then washed and incubated. Culture supernatants were collected at different time points, and then the cells were passaged if necessary. Levels of p24 antigen were measured using a Retro TEK p24 antigen ELISA kit, according to the manufacture's protocol. Signals were detected using an ELx808 microplate photometer.

For MT-4 Luc assays, MT-4 Luc cells (1×10^3 cells) grown in 96-well plates were infected with HIV-1_{XHB2} (ca. 0.2−10 ng p24) in the presence of varying concentrations of Vpr-3 R_8. At 6−7 d postinfection, cells were lysed and luciferase activity was measured using the Steady-Glo assay kits according to the manufacture's protocol. Chemiluminescence was detected with a Veritas luminometer.

Acknowledgment. We thank Prof. A. Iwamoto's group of the Institute of Medical Science at the University of Tokyo for the peptide libraries and Dr. M. Nicklaus from NCI/NIH for providing the modeled structure of full-length HIV-1 IN. T.T. is supported by JSPS research fellowships for young scientists.

This work was supported in part by Grant-in-Aid for Scientific Research from the Ministry of Education, Culture, Sports, Science, and Technology of Japan, and Health and Labor Sciences Research Grants from Japanese Ministry of Health, Labor, and Welfare. K.M. and Y.P. are supported by the Intramural Program of the National Cancer Institute, Center for Cancer Research.

Supporting Information Available: Additional experimental procedures including MS data and figures; HPLC charts of final compounds, explanation for HIV-1 genes and the peptide pools, and illustration of MT-4 Luc system. This material is available free of charge via the Internet at http://pubs.acs.org.

References

(1) Bukrinsky, M. I.; Haggerty, S.; Dempsey, M. P.; Sharova, N.; Adzhubei, A.; Spitz, L.; Lewis, P.; Goldfarb, D.; Emerman, M.; Stevenson, M. A nuclear-localization signal within HIV-1 matrix protein that governs infection of nondividing cells. *Nature* **1993**, *365*, 666–669.

(2) Miller, M. D.; Farnet, C. M.; Bushman, F. D. Human immunodeficiency virus type 1 preintegration complexes: studies of organization and composition. *J. Virol.* **1997**, *71*, 5382–5390.

(3) Farnet, C. M.; Bushman, F. D. HIV-1 cDNA integration: Requirement of HMG I(Y) protein for function of preintegration complexes in vitro. *Cell* **1997**, *88*, 483–492.

(4) Chen, H.; Engelman, A. The barrier-to-autointegration protein is a host factor for HIV type 1 integration. *Proc. Natl. Acad. Sci. U.S. A.* **1998**, *95*, 15270–15274.

(5) Gleenberg, I. O.; Herschhorn, A.; Hizi, A. Inhibition of the activities of reverse transcriptase and integrase of human immunodeficiency virus type-1 by peptides derived from the homologous viral protein R (Vpr). *J. Mol. Biol.* **2007**, *369*, 1230–1243.

(6) Gleenberg, I. O.; Avidan, O.; Goldgur, Y.; Herschhorn, A.; Hizi, A. Peptides derived from the reverse transcriptase of human immunodeficiency virus type 1 as novel inhibitors of the viral integrase. *J. Biol. Chem.* **2005**, *280*, 21987–21996.

(7) Hehl, E. A.; Joshi, P.; Kalpana, G. V.; Prasad, V. R. Interaction between human immunodeficiency virus type I reverse transcriptase and integrase proteins. *J. Virol.* **2004**, *78*, 5056–5067.

(8) Tasara, T.; Maga, G.; Hottiger, M. O.; Hubscher, U. HIV-1 reverse transcriptase and integrase enzymes physically interact and inhibit each other. *FEBS Lett.* **2001**, *507*, 39–44.

(9) Gleenberg, I. O.; Herschhorn, A.; Goldgur, Y.; Hizi, A. Inhibition of human immunodeficiency virus type-1 reverse transcriptase by a novel peptide derived from the viral integrase. *Arch. Biochem. Biophys.* **2007**, *458*, 202–212.

(10) Bischerour, J.; Tauc, P.; Leh, H.; De Rocquigny, H.; Roques, B.; Mouscadet, J. F. The (52−96) C-Terminal domain of Vpr stimulates HIV-1 IN-mediated homologous strand transfer of mini-viral DNA. *Nucleic Acids Res.* **2003**, *31*, 2694–2702.

(11) Hayouka, Z.; Rosenbluh, J.; Levin, A.; Loya, S.; Lebendiker, M.; Veprintsev, D.; Kotler, M.; Hizi, A.; Loyter, A.; Friedler, A. Inhibiting HIV-1 integrase by shifting its oligomerization equilibrium. *Proc. Natl. Acad. Sci. U.S.A.* **2007**, *104*, 8316–8312.

(12) Yan, H.; Mizutani, T. C.; Nomura, N.; Tanaka, T.; Kitamura, Y.; Miura, H.; Nishizawa, M.; Tatsumi, M.; Yamamoto, N.; Sugiura, W. A novel small molecular weight compound with a carbazole structure that demonstrates potent human immunodeficiency virus type-1 integrase inhibitory activity. *Antivir. Chem. Chemother.* **2005**, *16*, 363–373.

(13) Suzuki, T.; Futaki, S.; Niwa, M.; Tanaka, S.; Ueda, K.; Sugiura, Y. Possible existence of common internalization mechanisms among arginine-rich peptides. *J. Biol. Chem.* **2002**, *277*, 2437–2443.

(14) Wender, P. A.; Mitchell, D. J.; Pattabiraman, K.; Pelkey, E. T.; Steinman, L.; Rothbard, J. B. The design, synthesis, and evaluation of molecules that enable or enhance cellular uptake: Peptoid molecular transporters. *Proc. Natl. Acad. Sci. U.S.A.* **2000**, *97*, 13003–13008.

(15) Matsushita, M.; Tomizawa, K.; Moriwaki, A.; Li, S. T.; Terada, H.; Matsui, H. A high-efficiency protein transduction system demonstrating the role of PKA in long-lasting long-term potentiation. *J. Neurosci.* **2001**, *21*, 6000–6007.

(16) Takenobu, T.; Tomizawa, K.; Matsushita, M.; Li, S. T.; Moriwaki, A.; Lu, Y. F.; Matsui, H. Development of p53 protein transduction therapy using membrane-permeable peptides and the application to oral cancer cells. *Mol. Cancer Ther.* **2002**, *1*, 1043–1049.

(17) Wu, H. Y.; Tomizawa, K.; Matsushita, M.; Lu, Y. F.; Li, S. T.; Matsui, H. Poly-arginine-fused calpastatin peptide, a living cell membrane-permeable and specific inhibitor for calpain. *Neurosci. Res.* **2003**, *47*, 131–135.

(18) Rothbard, J. B.; Garlington, S.; Lin, Q.; Kirschberg, T.; Kreider, E.; McGrane, P. L.; Wender, P. A.; Khavari, P. A. Conjugation of arginine oligomers to cyclosporin A facilitates topical delivery and inhibition of inflammation. *Nature Med.* **2000**, *6*, 1253–1257.

(19) Marchand, C.; Zhang, X.; Pais, G. C. G.; Cowansage, K.; Neamati, N.; Burke, T. R., Jr.; Pommier, Y. Structural determinants for HIV-1 integrase inhibition by beta-diketo acids. *J. Biol. Chem.* **2002**, *277*, 12596–12603.

(20) Semenova, E. A.; Johnson, A. A.; Marchand, C.; Davis, D. A.; Tarchoan, R.; Pommier, Y. Preferential inhibition of the magnesium-dependent strand transfer reaction of HIV-1 integrase by alpha-hydroxytropolones. *Mol. Pharmacol.* **2006**, *69*, 1454–1460.

(21) Parniak, M. A.; Min, K. L.; Budihas, S. R.; Le Grice, S. F. J.; Beutler, J. A. A fluorescence-based high-throughput screening assay for inhibitors of HIV-1 reverse transcriptase associated ribonuclease H activity. *Anal. Biochem.* **2003**, *322*, 33–39.

(22) Morellet, N.; Bouaziz, S.; Petitjean, P.; Roques, B. P. NMR structure of the HIV-1 regulatory protein Vpr. *J. Mol. Biol.* **2003**, *327*, 215–227.

(23) Karki, R. G.; Tang, Y.; Burke, T. R., Jr.; Nicklaus, M. C. Model of full-length HIV-1 integrase complexed with viral DNA as template for anti-HIV drug design. *J. Comput.-Aided Mol. Des.* **2004**, *18*, 739–760.

(24) Wallace, A. C.; Laskowski, R. A.; Thormton, J. M. LIGPLOT—a program to generate schematic diagrams of protein ligand interactions. *Protein Eng.* **1995**, *8*, 127–134.

(25) Li, H.-Y.; Zawahir, Z.; Song, L.-D.; Long, Y.-Q.; Neamati, N. Sequence-based design and discovery of peptide inhibitors of HIV-1 integrase: insight into the binding mode of the enzyme. *J. Med. Chem.* **2006**, *49*, 4477–4486.

Bioorganic & Medicinal Chemistry 18 (2010) 6771–6775

Contents lists available at ScienceDirect

Bioorganic & Medicinal Chemistry

journal homepage: www.elsevier.com/locate/bmc

Peptidic HIV integrase inhibitors derived from HIV gene products: Structure–activity relationship studies

Shintaro Suzuki [a], Kasthuraiah Maddali [b], Chie Hashimoto [a], Emiko Urano [c], Nami Ohashi [a], Tomohiro Tanaka [a], Taro Ozaki [a], Hiroshi Arai [a], Hiroshi Tsutsumi [a], Tetsuo Narumi [a], Wataru Nomura [a], Naoki Yamamoto [c,d], Yves Pommier [b], Jun A. Komano [c], Hirokazu Tamamura [a,*]

[a] Institute of Biomaterials and Bioengineering, Tokyo Medical and Dental University, Chiyoda-ku, Tokyo 101-0062, Japan
[b] Laboratory of Molecular Pharmacology, Center for Cancer Research, National Cancer Institute, National Institutes of Health, Bethesda, MD 20892-4255, USA
[c] AIDS Research Center, National Institute of Infectious Diseases, Shinjuku-ku, Tokyo 162-8640, Japan
[d] Department of Microbiology, Yong Loo Lin School of Medicine, National University of Singapore, Singapore 117597, Singapore

ARTICLE INFO

Article history:
Received 28 June 2010
Revised 17 July 2010
Accepted 20 July 2010
Available online 25 July 2010

Keywords:
HIV integrase
Inhibitory peptide
Glu-Lys pairs
Ala-scan

ABSTRACT

Structure–activity relationship studies were conducted on HIV integrase (IN) inhibitory peptides which were found by the screening of an overlapping peptide library derived from HIV-1 gene products. Since these peptides located in the second helix of Vpr are considered to have an α-helical conformation, Glu-Lys pairs were introduced into the *i* and *i* + 4 positions to increase the helicity of the lead compound possessing an octa-arginyl group. Ala-scan was also performed on the lead compound for the identification of the amino acid residues responsible for the inhibitory activity. The results indicated the importance of an α-helical structure for the expression of inhibitory activity, and presented a binding model of integrase and the lead compound.

1. Introduction

Highly active anti-retroviral therapy (HAART), which involves a combination of two or three agents from two categories, reverse transcriptase inhibitors and protease inhibitors, has brought us remarkable success in the clinical treatment of HIV-infected and AIDS patients.[1] However, it has been accompanied by serious clinical problems including the emergence of viral strains with multidrug resistance (MDR), considerable adverse effects and nonetheless high costs. As a result, new categories of anti-HIV agents operating with mechanisms of action different from those of the above inhibitors are sought. HIV-1 integrase (IN) is a critical enzyme for the stable infection of host cells since it catalyzes the insertion of viral DNA into the genome of host cells, by means of strand transfer and 3′-end processing reactions and thus it is an attractive target for the development of anti-HIV agents. Recently, the first IN inhibitor, raltegravir (Merck),[2] has appeared in a clinical setting. It is assumed that the activity of IN must be negatively regulated during the translocation of the viral DNA from the cytoplasm to the nucleus to prevent auto-integration. The virus, as well as the host cells, must encode mechanism(s) to prevent auto-integration since the regulation of IN activity is critical for the virus to infect cells.[3] By screening a library of overlapping peptides derived from HIV-1 SF2 gene products we have found three Vpr-derived peptides, **1**, **2** and **3**, which possess significant IN inhibitory activity, indicating that IN inhibitors exist in the viral pre-integration complex (PIC).[4] The above inhibitory peptides, **1**, **2** and **3**, are consecutive overlapping peptides (Fig. 1). Compounds **4** and **5** are 12- and 18-mers from the original Vpr-sequence with the addition of an octa-arginyl group[5] into the C-terminus for cell membrane permeability, respectively. Compounds **4** and **5** have IN inhibitory activity and anti-HIV activity. Here, we report structure–activity relationship studies on these lead compounds for the development of more potent IN inhibitors.

2. Results and discussion

To determine which lead compound is most suitable for further experiments, five peptides **6–10**, which were elongated by one amino acid starting with compound **4** and extended ultimately to **5**, were synthesized (Fig. 2). Judging by the 3′-end processing and strand transfer reactions in vitro,[6] these peptides **4–10** had similar inhibitory potencies (Table 1). As a result, we concluded that 12 amino acid residues derived from the original Vpr-sequence are of sufficient for IN inhibitory activity, and any peptide among **4–10** is a suitable lead.

* Corresponding author.
E-mail address: tamamura.mr@tmd.ac.jp (H. Tamamura).

0968-0896/$ - see front matter © 2010 Elsevier Ltd. All rights reserved.
doi:10.1016/j.bmc.2010.07.050

1 AGVEAIIRILQQLLF
2 IIRILQQLLFIHFRI
3 LQQLLFIHFRIGCQH
4 Ac-LQQLLFIHFRIG-RRRRRRRR-NH_2
5 Ac-EAIIRILQQLLFIHFRIG-RRRRRRRR-NH_2

Figure 1. Amino acid sequences of compounds **1–5**. Compounds **1–3** are consecutive overlapping peptides with free N-/C-terminus. These were found by the IN inhibitory screening of a peptide library derived from HIV-1 gene products. Compounds **4** and **5** are cell penetrative leads of IN inhibitors.

4 Ac-LQQLLFIHFRIG-RRRRRRRR-NH_2
6 Ac-ILQQLLFIHFRIG-RRRRRRRR-NH_2
7 Ac-RILQQLLFIHFRIG-RRRRRRRR-NH_2
8 Ac-IRILQQLLFIHFRIG-RRRRRRRR-NH_2
9 Ac-IIRILQQLLFIHFRIG-RRRRRRRR-NH_2
10 Ac-AIIRILQQLLFIHFRIG-RRRRRRRR-NH_2
5 Ac-EAIIRILQQLLFIHFRIG-RRRRRRRR-NH_2

Figure 2. Amino acid sequences of compounds **6–10**, which are elongated by one amino acid from compound **4** to **5**.

Table 1
IC_{50} values of compounds **4–10** toward the 3′-end processing and strand transfer reactions catalyzed by HIV-1 IN

Compound	IC_{50} (μM)	
	3′-End processing	Strand transfer
4	0.13 ± 0.02	0.06 ± 0.01
5	0.09 ± 0.01	0.04 ± 0.01
6	0.10 ± 0.01	0.07 ± 0.01
7	0.13 ± 0.02	0.11 ± 0.01
8	0.26 ± 0.04	0.11 ± 0.03
9	0.11 ± 0.01	0.07 ± 0.01
10	0.08 ± 0.01	0.05 ± 0.01

Structural analysis showed that the Vpr-derived peptides, **1**, **2** and **3**, are located in the second helix of Vpr and were thus considered to have an α-helical conformation.[7] Compound **5** was adopted as a lead for the development of compounds with an increase in α-helicity since a longer peptide is likely to form a more stable α-helical structure than a shorter one. Initially, Glu (E) and Lys (K) were introduced in pairs into compound **5** at the i and $i+4$ positions. In general, such disposition of Glu-Lys pairs at i and $i+4$ positions is considered to cause an increase in α-helicity due to formation of an ionic interaction of a β-carboxy group of Glu and an ε-amino group of Lys. Several analogs of **5** with Glu-Lys pairs were synthesized by Fmoc-solid phase peptide synthesis (Fig. 3). In the inhibitory assay against the 3′-end processing and strand transfer reactions catalyzed by HIV-1 IN in vitro, compounds **11** and **15** showed more potent inhibitory activities than **5** (Table 2). Substitution of Glu-Lys for His^{14}-Gly^{18} or Ile^3-Leu^7 caused no decrease in IN inhibitory activity but a significant increase in activity, suggesting that Ile^3, Leu^7, His^{14} and Gly^{18} are not indispensable for activity. Substitution of Glu-Lys for Ala^2-Ile^6 or Gln^9-Ile^{13} caused a slight decrease in IN inhibitory activity against the 3′-end processing and strand transfer reactions (compounds **12** and **13**), indicating that Ala^2 and/or Ile^6, and Gln^9 and/or Ile^{13} are partly required for activity. Substitution of Glu-Lys for Ile^4-Gln^8 caused a 2–4-fold decrease in IN inhibitory activity against the 3′-end processing and strand transfer reactions (compound **14**), showing that Ile^4 and/or Gln^8 are essential for activity. Substitution of Glu-Lys for Leu^{11}-Phe^{15} caused an eightfold decrease in IN inhibitory activity against the 3′-end processing reaction and a 1.5-fold decrease in IN inhibitory activity against the strand transfer reaction (compound **16**), indicating that Leu^{11} and/or Phe^{15} are indispensable for activity, especially for inhibition against 3′-end processing. Compound **17** has two substitutions of Glu-Lys for His^{14}-Gly^{18} and for Ala^2-Ile^6, which are common to compounds **11** and **12**, respectively. A twofold decrease in both IN inhibitory activities of compound **17** is mostly due to the substitution for Ala^2-Ile^6 common to **12**, although **17** is slightly less active than **12** in both IN inhibitory assays.

1 5 10 15
5 Ac-EAIIRILQQLLFIHFRIG-RRRRRRRR-NH_2
11 Ac-EAIIRILQQLLFI<u>E</u>FRI<u>K</u>-RRRRRRRR-NH_2
12 Ac-E<u>E</u>IIR<u>K</u>LQQLLFIHFRIG-RRRRRRRR-NH_2
13 Ac-EAIIRILQ<u>E</u>LLF<u>K</u>HFRIG-RRRRRRRR-NH_2
14 Ac-EAI<u>E</u>RIL<u>K</u>QLLFIHFRIG-RRRRRRRR-NH_2
15 Ac-EA<u>E</u>IRI<u>K</u>QQLLFIHFRIG-RRRRRRRR-NH_2
16 Ac-EAIIRILQQL<u>E</u>FIH<u>K</u>RIG-RRRRRRRR-NH_2
17 Ac-E<u>E</u>IIR<u>K</u>LQQLLFI<u>E</u>FRI<u>K</u>-RRRRRRRR-NH_2

Figure 3. Amino acid sequences of compounds **11–17**, into which Glu-Lys pairs have been introduced.

Table 2
IC_{50} values of compounds **5** and **11–17** toward the 3′-end processing and strand transfer reactions catalyzed by HIV-1 IN

Compound	IC_{50} (μM)	
	3′-End processing	Strand transfer
5	0.09 ± 0.01	0.04 ± 0.01
11	0.05 ± 0.01	0.01 ± 0.001
12	0.12 ± 0.01	0.047 ± 0.01
13	0.14 ± 0.02	0.065 ± 0.01
14	0.23 ± 0.03	0.15 ± 0.002
15	0.04 ± 0.01	0.031 ± 0.01
16	0.71 ± 0.21	0.06 ± 0.004
17	0.18 ± 0.06	0.08 ± 0.02

Anti-HIV activity of these compounds was assessed by an MT-4 Luc system, in which MT-4 cells were stably transduced with the firefly luciferase expression cassette by a murine leukemia viral vector. MT-4 Luc cells constitutively express high levels of luciferase. HIV-1 infection significantly reduces luciferase expression due to the high susceptibility of MT-4 cells to HIV-1 infection. Protection of MT-4 Luc cells from HIV-1-induced cell death maintains the luciferase signals at high levels. In addition, the cytotoxicity of test compounds can be evaluated by a decrease of luciferase signals in these MT-4 Luc systems. The parent compound **5** showed significant anti-HIV activity at concentrations above 1.25 μM, as reported previously (Fig. 4).[4] Compound **15** showed a significant inhibitory effect against HIV-1 replication, and is thus comparable to compound **5**. Compounds **11**, **14** and **16** also displayed weak antiviral effects at concentrations of 2.5 and 5.0 μM and compounds **12**, **13** and **17** failed to show any significant anti-HIV activity. These results suggest that there is a positive correlation between IN inhibitory activity and anti-HIV activity of the compounds. None of these compounds showed significant cytotoxic effects at concentrations below 5.0 μM.

The structures of compounds **5** and **11–17** were assessed by CD spectroscopy. Because the aqueous solubility of these peptides is not high the peptides were dissolved in 0.1 M phosphate buffer, containing 50% MeOH at pH 5.6. The CD spectra suggest that the parent compound **5**, which has no Glu-Lys pair, forms a typical α-helical structure, and the other compounds, with the exception of **11** and **15**, form α-helical structures similarly (Fig. 5). The order of strength of α-helicity is **12**, **16** > **14** > **17** > **5** > **13**. Compounds **11** and **15** have no characteristic pattern, although IN inhibitory activities of both compounds are superior to that of the parent

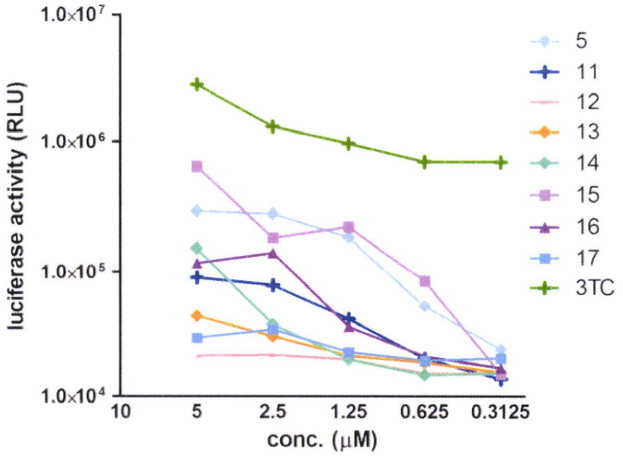

Figure 4. Luciferase signals in MT-4 Luc cells infected with HIV-1 in the presence of different concentrations of compounds **11–17**. Luciferase activity is expressed as relative luciferase units (RLU). 3TC is an HIV reverse transcriptase inhibitor, which was used as a positive control.

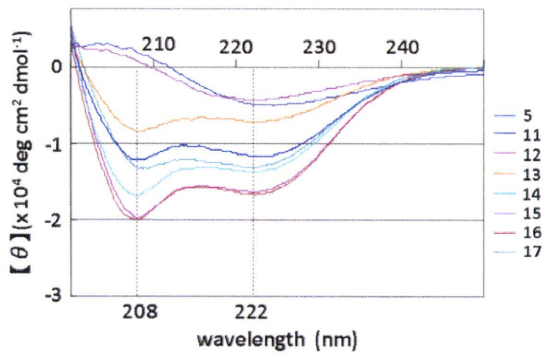

Figure 5. CD spectra of compounds **5** and **11–17** (5 μM) in 0.1 M phosphate buffer, pH 5.6 containing 50% MeOH at 25 °C.

compound **5**. Replacement of His^{14}-Gly^{18} and Ile^{3}-Leu^{7} by Glu-Lys in compounds **11** and **15**, respectively, caused a significant decrease in α-helicity, possibly due to formation of unfavorable salt bridges such as Glu^{14}-Arg^{16} and Glu^{3}-Arg^{5}. Introduction of a Glu-Lys pair into Gln^{9}-Ile^{13} in compound **13** caused a slight decrease in α-helicity, possibly due to interference in the formation of a salt bridge of Glu^{1}-Arg^{5} by that of Arg^{5}-Glu^{9}. In the other analogs, increases in α-helicity were observed to result from the introduction of Glu-Lys pairs as we had initially postulated. Overall, there is no positive correlation between IN inhibitory or anti-HIV activity and the degree of α-helicity of the compounds.

In order to identify the amino acid residues responsible for IN inhibitory and anti-HIV activities of these peptides, an Ala-scan of compound **4** was performed (Fig. 6). Compounds **18–22**, **25**, **27** and **29** showed IN inhibitory activities against the 3′-end processing and strand transfer reactions similar to those of **4** (Table 3). Ala-substitution for Leu^{7}, Gln^{8}, Gln^{9}, Leu^{10}, Leu^{11}, His^{14}, Arg^{16} or Gly^{18} did not cause any significant change in either of IN inhibitory activities, indicating that the replaced amino acids are not essential for IN inhibition. Ala-substitution for Phe^{12}, Ile^{13}, Phe^{15} or Ile^{17} gave compounds **23**, **24**, **26** and **28**, which were 2–4 times less active in both the IN inhibitory assays, suggesting that Phe^{12}, Ile^{13}, Phe^{15} and Ile^{17} are indispensable for IN inhibition. Assessment of anti-HIV activity in the MT-4 Luc system showed that all compounds **18–29** produced dose-dependent inhibition of HIV-1 replication, although they displayed cytotoxicity at 10 μM (**4**, **19–23**, **26** and **27**) or above 5 μM (**24** and **25**) (Fig. 7). Compounds **23** and **24**,

7 10 15

4	Ac-LQQLLFIHFRIG-RRRRRRRR-NH_2
18	Ac-AQQLLFIHFRIG-RRRRRRRR-NH_2
19	Ac-LAQLLFIHFRIG-RRRRRRRR-NH_2
20	Ac-LQALLFIHFRIG-RRRRRRRR-NH_2
21	Ac-LQQALFIHFRIG-RRRRRRRR-NH_2
22	Ac-LQQLAFIHFRIG-RRRRRRRR-NH_2
23	Ac-LQQLLAIHFRIG-RRRRRRRR-NH_2
24	Ac-LQQLLFAHFRIG-RRRRRRRR-NH_2
25	Ac-LQQLLFIAFRIG-RRRRRRRR-NH_2
26	Ac-LQQLLFIHARIG-RRRRRRRR-NH_2
27	Ac-LQQLLFIHFAIG-RRRRRRRR-NH_2
28	Ac-LQQLLFIHFRAG-RRRRRRRR-NH_2
29	Ac-LQQLLFIHFRIA-RRRRRRRR-NH_2

Figure 6. Amino acid sequences of compounds **18–29** based on an Ala-scan of compound **4**. Position numbers correspond to alignment with compound **5**.

Table 3
IC_{50} values of compounds **18–29** toward the 3′-end processing and strand transfer reactions catalyzed by HIV-1 IN

Compound	IC_{50} (μM)	
	3′-End processing	Strand transfer
4	0.11 ± 0.03	0.05 ± 0.01
18	0.12 ± 0.004	0.08 ± 0.01
19	0.13 ± 0.02	0.06 ± 0.01
20	0.10 ± 0.004	0.06 ± 0.01
21	0.12 ± 0.02	0.07 ± 0.01
22	0.13 ± 0.003	0.06 ± 0.01
23	0.34 ± 0.06	0.18 ± 0.03
24	0.33 ± 0.02	0.22 ± 0.01
25	0.13 ± 0.01	0.06 ± 0.01
26	0.25 ± 0.02	0.12 ± 0.01
27	0.11 ± 0.01	0.05 ± 0.01
28	0.20 ± 0.03	0.16 ± 0.02
29	0.09 ± 0.01	0.09 ± 0.01

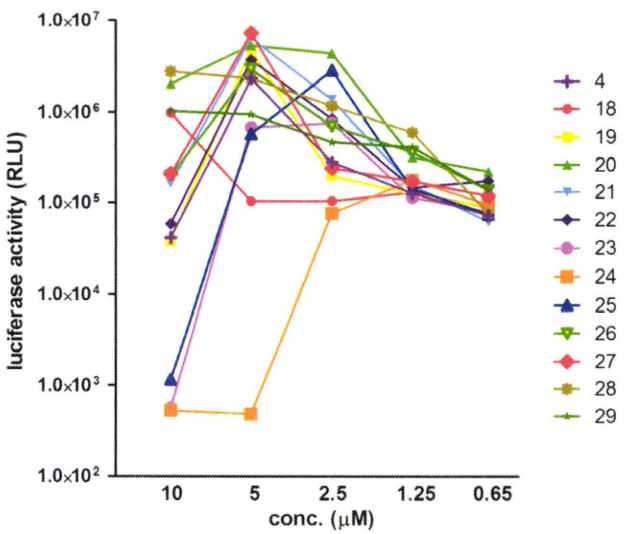

Figure 7. Luciferase signals in MT-4 Luc cells infected with HIV-1 in the presence of various concentrations of compounds **18–29**. Luciferase activity was valued as RLU.

with Ala-substitution for Phe^{12} and Ile^{13}, respectively, showed weaker inhibitory activity than **4** at 5 μM. Consequently, Phe^{12} and Ile^{13} were deemed to be critical for activity, which is consistent with the IN inhibitory activity results. A control peptide isomer of **5** (Ac-QIFEHLAGIIQILRFLRI-R_8-NH_2) did not show anti-HIV activity at

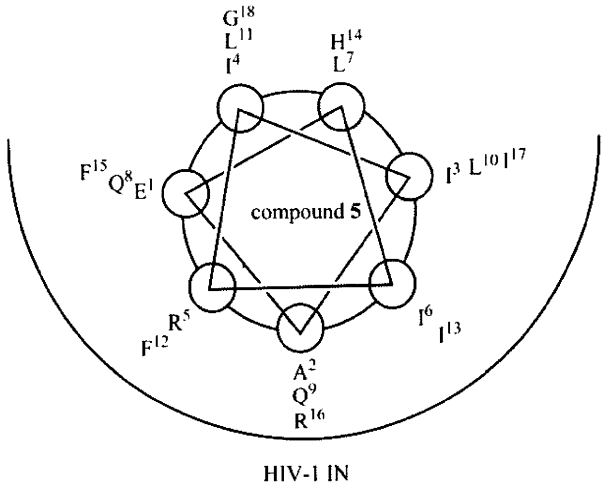

Figure 8. Brief presumed drawing of the binding model of HIV-1 IN and compound **5**.

concentrations below 10 μM, suggesting that the original Vpr-sequence, with the exceptions of Phe^{12}, Ile^{13}, Phe^{15} and Ile^{17}, is critical for activity.

The assumption that compound **5** forms an α-helical structure when binding to HIV-1 IN suggests the binding model of IN and **5** shown in Figure 8, as **5** forms an α-helical structure in 50% aqueous MeOH solution. In this model, Phe^{12}, Ile^{13}, Phe^{15} and Ile^{17}, which were identified by the Ala-scan experiment as critical residues, are located in the pocket of IN. His^{14} and Gly^{18}, which can be replaced by Glu-Lys with an increase of activity in compound **11**, are located outside of the pocket of IN. Ile^{3} and Leu^{7} can also be replaced by Glu-Lys while retaining activity in compound **15**, and Leu^{7} is located outside of the pocket, whereas Ile^{3} is located in the edge of the pocket. Compounds **11** and **15** might form α-helical structures when binding to IN, although **11** or **15** does not show α-helicity in the CD spectrum. Thus, these compounds might retain IN inhibitory activity. This binding model is compatible with the results of structure–activity relationship studies involving Glu-Lys substitution and Ala-scan. The reason for decreases in IN inhibitory and anti-HIV activity of compounds **12** and **17**, which show increases of α-helicity, are possibly due to substitution of Glu-Lys for Ala^{2} and Ile^{6}, which are located in the pocket of IN. The reason for a decrease in activity of compounds **14** and **16**, which show increased α-helicity, might be due to substitution of Lys for Gln^{8} and Phe^{15}, respectively, which are located in the pocket of IN. The reason for decreases in IN inhibitory and anti-HIV activity of compound **13**, which also shows a decrease of α-helicity, are possibly due to substitution of Glu-Lys for Gln^{9} and Ile^{13}, which are located in the pocket of IN.

3. Conclusion

In the present study, structure–activity relationship studies were performed on Vpr-derived peptides **4** and **5**, which had been previously identified as HIV-1 IN inhibitors.[4] The Glu-Lys substitution experiments and Ala-scan data suggest that several amino acid residues of **4** and **5** are indispensable for IN inhibitory and anti-HIV activities, and a binding model of IN and **5** were proposed. Furthermore, two novel compounds **11** and **15**, which contained Glu-Lys pairs and showed more potent IN inhibitory activities than compound **5**, were found. These data including the binding model should be useful for the development of potent HIV-1 IN inhibitors based on Vpr-peptides.

4. Experimental

4.1. Chemistry

All peptides were synthesized by the Fmoc-based solid-phase method. The synthetic peptides were purified by RP-HPLC and identified by ESI-TOF-MS. Fmoc-protected amino acids and reagents for peptide synthesis were purchased from Novabiochem, Kokusan Chemical Co., Ltd and Watanabe Chemical Industries, Ltd. Protected peptide resins were constructed on NovaSyn TGR resins (0.26 meq/g, 0.025 and 0.0125 mmol scales for Glu-Lys substitution and Ala-scan peptides, respectively). All peptides were synthesized by stepwise elongation techniques. Each cycle involves (i) deprotection of an Fmoc group with 20% (v/v) piperidine/DMF (10 mL) for 15 min and (ii) coupling with 5.0 equiv of Fmoc-protected amino acid, 5.0 equiv of diiopropylcarbodiimide (DIPCI) and 5.0 equiv of 1-hydroxybenzotriazole monohydrate ($HOBt{\cdot}H_2O$) in DMF (3 mL) for 90 min. N-Terminal α-amino groups of Glu-Lys substitution and Ala-scan peptides were acetylated with 100 equiv of acetic anhydride in DMF (10 mL). Cleavage from the resin and side chain deprotection were carried out by stirring for 1.5 h with *m*-cresol (0.25 mL), thioanisole (0.75 mL), 1,2-ethanedithiol (0.75 mL) and TFA (8.25 mL). After removal of the resins by filtration, the filtrate was concentrated under reduced pressure, the crude peptides were precipitated in cooled diethyl ether and purified by preparative RP-HPLC on a Cosmosil 5C18-AR II column (10 × 250 mm, Nacalai Tesque, Inc.) with a LaChrom Elite HTA system (Hitachi). The HPLC solvents employed were water containing 0.1% TFA (solvent A) and acetonitrile containing 0.1% TFA (solvent B). All peptides were purified using a linear gradient of solvents A and B over 30 min at a flow rate of 3 $cm^3\ min^{-1}$. The purified peptides were identified by ESI-TOF-MS (Brucker Daltonics micrOTOF-2focus) (shown in Table S1 in Supplementary data). All peptides were obtained after lyophilization as fluffy white powders of the TFA salts. The purities of these peptides were checked by analytical HPLC on a Cosmosil 5C18-ARII column (4.6 × 250 mm, Nacalai Tesque, Inc.) eluted with a linear gradient of solvents A and B at a flow rate of 1 $cm^3\ min^{-1}$, and eluted products were detected by UV at 220 nm (shown in Figs. S1–S3 in Supplementary data).

4.2. Expression and purification of F185K/C280S HIV-1 integrase from *Escherichia coli*

Plasmid encoding IN1–288/F185K/C280S was expressed in *Escherichia coli* strain C41. The solubility of the mutant protein was examined in a crude cell lysate, as follows. Cells were grown in 1 L of culture medium containing 100 μg/mL of ampicillin at 37 °C until the optical density of the culture at 600 nm was between 0.4 and 0.9. Protein expression was induced by the addition of isopropyl-1-thio-β-D-galactopyranoside to a final concentration of 0.1 mM. After 2 h, the cells were collected by centrifugation at 6000 rpm for 30 min. After removal of the supernatant, the cells were resuspended in HED buffer (20 mM HEPES, pH 7.5, 1 mM EDTA, 1 mM DTT) with 0.5 mg/mL lysozyme and stored on ice for 30 min. The cells were sonicated until the solution exhibited minimal viscosity then it was centrifuged at 15,000 rpm for 30 min. After removal of the supernatant, the pellet was dissolved in TNM buffer (20 mM Tris/HCl, pH 8.0, 1 M NaCl, 2 mM 2-mercaptoethanol) with 5 mM imidazole and stored on ice for 30 min. The cells were then centrifuged at 15,000 rpm for 30 min and the supernatant was collected. The supernatant was then filtered through 0.45 μm filter cartridge and applied to a HisTrap column at 1 mL/min flow rate. After loading, the column was washed with 10 volume of TNM buffer with 5 mM imidazole. Protein was eluted with a linear gradient of 500 mM imidazole, containing TNM buf-

fer. Fractions containing IN were pooled and checked with SDS–PAGE.

4.3. CD spectroscopy of peptides with Glu-Lys substitution

CD measurements were performed on a JASCO J720 spectropolarimeter equipped with thermo-regulator (JASCO Corp., Ltd), using 5 μM of peptides dissolved in 0.1 M phosphate buffer, pH 5.6 containing 50% MeOH. UV spectra were recorded at 25 °C in a quartz cell 1.0 mm path length, a time constant of 1 s, and a 100 nm/min scanning speed with 0.1 nm resolution.

4.4. Integrase assays

Expression and purification of the recombinant IN in *E. coli* were performed as previously reported with addition of 10% glycerol to all buffers. Oigonucleotide substrates were prepared as described.[6] Integrase reactions were performed in 10 μL with 400 nM of recombinant IN, 20 nM of 5′-end [^{32}P]-labeled oligonucleotide substrate and inhibitors at various concentrations. Solutions of 10% DMSO without inhibitors were used as controls. Reaction mixtures were incubated at 37 °C (60 min) in buffer containing 50 mM MOPS, pH 7.2, 7.5 mM $MgCl_2$, and 14.3 mM 2-mercaptoethanol. Reactions were stopped by addition of 10 μL of loading dye (10 mM EDTA, 98% deionized formamide, 0.025% xylene cyanol and 0.025% bromophenol blue). Reactions were then subjected to electrophoresis in 20% polyacrylamide–7 M urea gels. Gels were dried and reaction products were visualized and quantitated with a Typhoon 8600 (GE Healthcare, Little Chalfont, Buckinghamshire, UK). Densitometric analyses were performed using ImageQuant from Molecular Dynamics Inc. The concentrations at which enzyme activity was reduced by 50% (IC_{50}) were determined using 'Prism' software (GraphPad Software, San Diego, CA) for nonlinear regression to fit dose–response data to logistic curve models.

4.5. Replication assays (MT-4 luciferase assays)

MT-4 luciferase cells (1×10^3 cells) grown in 96-well plates were infected with HIV-1_{HXB2} in the presence of various concentrations of peptides. At 6–7 days post-infection, cells were lysed and the luciferase activities were measured using the Steady-Glo assay kit (Promega), according to the manufacturer's protocol. Chemiluminescence was detected with a Veritas luminometer (Promega).

Acknowledgments

N.O. and T.T. are supported by JSPS research fellowships for young scientists. This work was supported by Mitsui Life Social Welfare Foundation, Grant-in-Aid for Scientific Research from the Ministry of Education, Culture, Sports, Science, and Technology of Japan, the Health and Labour Sciences Research Grants from Japanese Ministry of Health, Labor, and Welfare, and by the NIH Intramural Program, Center for Cancer Research, US National Cancer Institute.

Supplementary data

Supplementary data associated with this article can be found, in the online version, at doi:10.1016/j.bmc.2010.07.050.

References and notes

1. Mitsuya, H.; Erickson, J. In *Textbook of AIDS Medicine*; Merigan, T C., Bartlett, J. G., Bolognesi, D., Eds.; Williams & Wilkins: Baltimore, 1999; pp 751–780.
2. (a) Cahn, P.; Sued, O. *Lancet* **2007**, *369*, 1235; (b) Grinsztejn, B.; Nguyen, B.-Y.; Katlama, C.; Gatell, J. M.; Lazzarin, A.; Vittecoq, D.; Gonzalez, C. J.; Chen, J.; Harvey, C. M.; Isaacs, R. D. *Lancet* **2007**, *369*, 1261.
3. (a) Farnet, C. M.; Bushman, F. D. *Cell* **1997**, *88*, 483; (b) Chen, H.; Engelman, A. *Proc. Natl. Acad. Sci. U.S.A.* **1998**, *95*, 15270; (c) Gleenberg, I. O.; Herschhorn, A.; Hizi, A. *J. Mol. Biol.* **2007**, *369*, 1230; (d) Gleenberg, I. O.; Avidan, O.; Goldgur, Y.; Herschhorn, A.; Hizi, A. *J. Biol. Chem.* **2005**, *280*, 21987; (e) Hehl, E. A.; Joshi, P.; Kalpana, G. V.; Prasad, V. R. *J. Virol.* **2004**, *78*, 5056; (f) Tasara, T.; Maga, G.; Hottiger, M. O.; Hubscher, U. *FEBS Lett.* **2001**, *507*, 39; (g) Gleenberg, I. O.; Herschhorn, A.; Goldgur, Y.; Hizi, A. *Arch. Biochem. Biophys.* **2007**, *458*, 202.
4. Suzuki, S.; Urano, E.; Hashimoto, C.; Tsutsumi, H.; Nakahara, T.; Tanaka, T.; Nakanishi, Y.; Maddali, K.; Han, Y.; Hamatake, M.; Miyauchi, K.; Pommier, Y.; Beutler, J. A.; Sugiura, W.; Fuji, H.; Hoshino, T.; Itotani, K.; Nomura, W.; Narumi, T.; Yamamoto, N.; Komano, J. A.; Tamamura, H. *J. Med. Chem.* **2010**, *53*, 5356.
5. Suzuki, T.; Futaki, S.; Niwa, M.; Tanaka, S.; Ueda, K.; Sugiura, Y. *J. Biol. Chem.* **2002**, *277*, 2437.
6. (a) Yan, H.; Mizutani, T. C.; Nomura, N.; Tanaka, T.; Kitamura, Y.; Miura, H.; Nishizawa, M.; Tatsumi, M.; Yamamoto, N.; Sugiura, W. *Antivir. Chem. Chemother.* **2005**, *16*, 363; (b) Marchand, C.; Zhang, X.; Pais, G. C. G.; Cowansage, K.; Neamati, N.; Burke, T. R., Jr.; Pommier, Y. *J. Biol. Chem.* **2002**, *277*, 12596; (c) Semenova, E. A.; Johnson, A. A.; Marchand, C.; Davis, D. A.; Tarchoan, R.; Pommier, Y. *Mol. Pharmacol* **2006**, *69*, 1454; (d) Leh, H.; Brodin, P.; Bischerour, J.; Deprez, E.; Tauc, P.; Brochon, J. C.; LeCam, E.; Coulaud, D.; Auclair, C.; Mouscadet, J. F. *Biochemistry* **2000**, *39*, 9285; (e) Marchand, C.; Neamati, N.; Pommier, Y. In Vitro Human Immunodeficiency Virus Type 1 Integrase Assays. In *Methods in Enzymology (Drug-Nucleic Acid Interactions)*; Chaires, J. B., Waring, M. J., Eds.; Elsevier: Amsterdam, 2001; Vol. 340, pp 624–633.
7. Morellet, N.; Bouaziz, S.; Petitjean, P.; Roques, B. P. *J. Mol. Biol.* **2003**, *327*, 215.

Bioorganic & Medicinal Chemistry Letters 20 (2010) 5853–5858

Contents lists available at ScienceDirect

Bioorganic & Medicinal Chemistry Letters

journal homepage: www.elsevier.com/locate/bmcl

CD4 mimics targeting the HIV entry mechanism and their hybrid molecules with a CXCR4 antagonist

Tetsuo Narumi [a], Chihiro Ochiai [a], Kazuhisa Yoshimura [b], Shigeyoshi Harada [b], Tomohiro Tanaka [a], Wataru Nomura [a], Hiroshi Arai [a], Taro Ozaki [a], Nami Ohashi [a], Shuzo Matsushita [b], Hirokazu Tamamura [a,*]

[a] Institute of Biomaterials and Bioengineering, Tokyo Medical and Dental University, Chiyoda-ku, Tokyo 101-0062, Japan
[b] Center for AIDS Research, Kumamoto University, Kumamoto 860-0811, Japan

ARTICLE INFO

Article history:
Received 14 June 2010
Revised 22 July 2010
Accepted 26 July 2010
Available online 3 August 2010

Keywords:
CD4
HIV entry
Hybrid molecule
gp120

ABSTRACT

Small molecules behaving as CD4 mimics were previously reported as HIV-1 entry inhibitors that block the gp120–CD4 interaction and induce a conformational change in gp120, exposing its co-receptor-binding site. A structure–activity relationship (SAR) study of a series of CD4 mimic analogs was conducted to investigate the contribution from the piperidine moiety of CD4 mimic **1** to anti-HIV activity, cytotoxicity, and CD4 mimicry effects on conformational changes of gp120. In addition, several hybrid molecules based on conjugation of a CD4 mimic analog with a selective CXCR4 antagonist were also synthesized and their utility evaluated.

The infection of host cells by HIV-1 takes place in multiple steps via a dynamic supramolecular mechanism mediated by two viral envelope glycoproteins (gp41, gp120) and several cell surface proteins (CD4, CCR5/CXCR4).[1] Cell penetration begins with the interaction of gp120 with the primary receptor CD4. This induces conformational changes in gp120, leading to the exposure of its V3 loop allowing the subsequent binding of gp120 to a co-receptor, CCR5[2] or CXCR4.[3]

N-(4-Chlorophenyl)-*N*′-(2,2,6,6-tetramethyl-piperidin-4-yl)oxalamide (NBD-556: **1**) and the related compounds NBD-557 (**2**) and YYA-021 (**3**) have been identified as a novel class of HIV-1 entry inhibitors, which exert potent cell fusion and virus cell fusion inhibitory activity at low micromolar levels (Fig. 1).[4] Furthermore, compound **1** can also induce thermodynamically favored conformational changes in gp120 similar to those caused by CD4 binding. The X-ray crystal structure of gp120 complexed with CD4 revealed the presence of a hydrophobic cavity, the Phe43 cavity, which is penetrated by the aromatic ring of Phe^{43} of CD4.[5] Molecular modeling revealed that compound **1** is also inserted into the Phe43 cavity, the *para*-chlorophenyl group of **1** entering more deeply than the phenyl ring of Phe^{43} of CD4 and interacting with the conserved gp120 residues such as Trp^{427}, Phe^{382}, and Trp^{112}.[4c] The modeling also suggested that an oxalamide linker forms hydrogen bonds with carbonyl groups of the gp120 backbone peptide bonds. Our model of **1** docked into gp120 revealed that eight other gp120 residues, Val^{255}, Asp^{368}, Glu^{370}, Ser^{375}, Ile^{424}, Trp^{427}, Val^{430}, and Val^{475} are located within a 4.4 Å-radius of **1** and that a large cavity exists around the *p*-position of the aromatic ring of **1**.[4e] Based on these observations, we conducted a structure–activity relationship (SAR) study of a series of analogs of CD4 mimics with substituents at the *p*-position of the aromatic ring. This study revealed that a certain size and electron-withdrawing ability of the substituents are indispensable for potent anti-HIV activity.[4e]

Although several reported SAR studies of **1** have revealed the contributions of the phenyl ring and the oxalamide linker of **1** to the binding affinity with gp120, the anti-HIV activity and the CD4 mimicry on conformational changes of gp120,[4] there has been, to the best of our knowledge, no prior report describing SAR studies of the piperidine ring of **1**. In this paper, the contributions of the piperidine ring of **1** to the anti-HIV activity, CD4 mimicry and cytotoxicity were investigated through the SAR studies focused on the piperidine ring of **1**. Furthermore, to apply the utility of CD4 mimics to the development of potent anti-HIV agents, a series of the

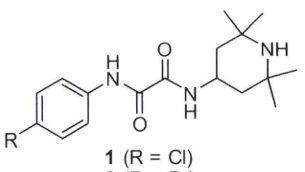

1 (R = Cl)
2 (R = Br)
3 (R = Me)

Figure 1. NBD-556 (**1**) and related compounds.

* Corresponding author.
E-mail address: tamamura.mr@tmd.ac.jp (H. Tamamura).

0960-894X/$ - see front matter © 2010 Elsevier Ltd. All rights reserved.
doi:10.1016/j.bmcl.2010.07.106

hybrid molecules that combined CD4 mimic analogs with a selective CXCR4 antagonist were also synthesized and bioevaluated.

For the design of novel CD4 mimic analogs, we initially tried to directly derivatize the nitrogen atom of piperidine group. However, direct alkylation and acylation of **1** failed probably as a result of steric hindrance from the methyl groups on the piperidine ring so we synthesized several derivatives lacking the methyl groups and evaluated their anti-HIV activity, cytotoxicity, and ability to mimic CD4. According to the previous SAR study,[4e] the *p*-Cl (**4**), *p*-Br (**5**) and *p*-methyl derivatives (**6**) lacking the methyl groups on the piperidine ring were prepared. Compounds **4–6** were synthesized by published methods as shown in Scheme 1. Briefly, coupling of aniline derivatives with ethyl chloroglyoxalate in the presence of Et_3N and subsequent saponification gave the corresponding acids (**10–12**). Condensation of these acids with 4-amino-*N*-benzylpiperidine in the presence of EDC–HOBt system, followed by debenzylation under von Braun conditions with 1-chloroethyl choroformate[6] produced the desired compounds **4–6**.[7]

The anti-HIV activity of each of the synthetic compounds was evaluated against MNA (R5) strain, with the results shown in Table 1. IC_{50} values were determined by the 3-(4,5-dimethylthiazol-2-yl)-2,5-diphenyltetrazolium bromide (MTT) method[8] as the concentrations of the compounds which conferred 50% protection against HIV-1-induced cytopathogenicity in PM1/CCR5 cells. Cytotoxicity of the compounds based on the viability of mock-infected PM1/CCR5 cells was also evaluated using the MTT method. CC_{50} values, the concentrations achieving 50% reduction of the viability of mock-infected cells, were also determined. Compounds **1** and **3** showed potent anti-HIV activity. The anti-HIV IC_{50} of compound **2** was previously reported to be comparable to that of compound **1**, and thus was not determined in this study. Novel derivatives **4** and **6** without the methyl groups on the piperidine ring, showed significant anti-HIV activity comparable to that of the parent compounds **1** and **3**, respectively. The *p*-methyl derivative **6** has slightly lower activity than the *p*-Cl derivative **4** and the *p*-Br derivative **5**. These results are consistent with our previous SAR studies on the parent compounds **1–3**. Compound **5** was found to exhibit relatively strong cytotoxicity (CC_{50} = 50 μM) and compounds **4** and **6** have cytotoxicities comparable to that of compounds **1** and **3**, respectively. This observation indicates that the methyl groups on the piperidine ring do not contribute significantly to the anti-HIV activity or the cytotoxicity.

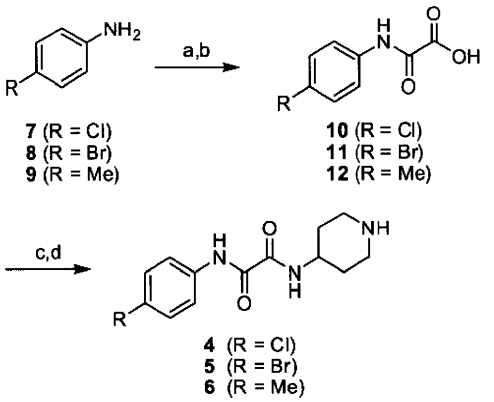

Scheme 1. Synthesis of compounds **4–6**. Reagents and conditions: (a) ethyl chloroglyoxylate, Et_3N, THF; (b) 1 M aq NaOH, THF, 67%–quant.; (c) 1-benzyl-4-aminopiperidine, EDC·HCl, HOBt·H_2O, Et_3N, THF; (d) (i) 1-chloroethyl chloroformate, CH_2Cl_2; (ii) MeOH, 8–47%.

Table 1
Effects of the methyl groups on anti-HIV activity and cytotoxicity of CD4 mimic analogs[a]

Compd	R	IC_{50} (μM) MNA (R5)	CC_{50} (μM)
1	Cl	12	110
2	Br	ND	93
3	Me	15	210
4	Cl	8	100
5	Br	6	50
6	Me	20	190

[a] All data with standard deviation are the mean values for at least three independent experiments (ND = not determined).

Compound **1** and the newly synthesized derivatives **4–6** were also evaluated for their effects on conformational changes of gp120 by a fluorescence activated cell sorting (FACS) analysis. The profile of binding of an anti-envelope CD4-induced monoclonal antibody (4C11) to the Env-expressing cell surface (an R5-HIV-1 strain, JR-FL, -infected PM1 cells) pretreated with the above derivatives was examined. Comparison of the binding of 4C11 to the cell surface was measured in terms of the mean fluorescence intensity (MFI), as shown in Figure 2. Pretreatment of the Env-expressing cell surface with compound **1** (MFI = 53.66) produced a significant increase in binding affinity for 4C11, consistent with that reported previously.[4e] This indicates that compound **1** enhances the binding affinity of gp120 with the 17b monoclonal antibody which recognizes CD4-induced epitopes on gp120. The Env-expressing cells without CD4 mimic-pretreatment failed to show significant binding affinity to 4C11. On the other hand, the profiles of the binding of 4C11 to the Env-expressing cell surface pretreated with compound **4** (Cl derivative) and **5** (Br derivative) (MFI = 49.88 and 52.34) were similar to that of compound **1**. Pretreatment of the cell surface with compound **6** (Me derivative) (MFI = 45.99) produced slightly lower enhancement but significant levels of binding affinity for 4C11, compared to that of compound **1** as pretreatments. These results suggested that the removal of the methyl groups on the piperidine moiety might not affect the CD4 mimicry effects on conformational changes of gp120 and it was conjectured that the phenyl ring of CD4 mimic might be a key moiety for the interaction with gp120 to induce the conformational changes of gp120. This is consistent with the results in the previous paper where it was reported that CD4 mimics having suitable substituent(s) on the phenyl ring cause a conformational change, resulting in external exposure of the co-receptor-binding site of gp120.[4e]

Based on these results, a series of N-alkylated and N-acylated piperidine derivatives **13–18** with no methyl groups were prepared. Several compounds with 6-membered rings were also prepared to determine whether or not the piperidine ring is mandatory. The synthesis of these derivatives is shown in Scheme 2. Since the *p*-Cl derivative **4** showed potent anti-HIV activity and relatively low cytotoxicity, compared to the *p*-Br derivative **5**, chlorine was selected as the substituent at the *p*-position of the phenyl ring. The N-methyl derivative **13** was synthesized by coupling of **10** with 4-amine-1-methylpiperidine. Alkylation of **4** with *tert*-butyl bromoacetate, followed by deprotection of *tert*-butyl ester provided compound **14**. The N-isopropyl derivative **15** was prepared by reductive amination of **4** with isopropyl aldehyde. The N-acyl derivatives **16–18** were prepared by simple acylation or condensation with the corresponding substrate. The synthesis of other derivatives **19–23** with different 6-membered rings is depicted in Scheme 3. The 6-membered ring derivatives with the exception of **21** were prepared by coupling of acid **10** with the corresponding amines. Compound **21** was prepared by reaction of **10** with thionyl chloride to give the corresponding acid chloride, which was subsequently coupled with 4-aminopyridine.

Compounds **1**, **3**, and **13–18** were evaluated for their CD4 mimicry effects on conformational changes of gp120 by the FACS anal-